

## Supporting Information for

# Alkaline-earth metal embedded expanded phthalocyanine nanosheets with direct band gap and high power conversion efficiency

Cui Wang and Li-Ming Yang\*

*Key Laboratory of Material Chemistry for Energy Conversion and Storage, Ministry of Education, Hubei Key Laboratory of Materials Chemistry and Service Failure, Hubei Key Laboratory of Bioinorganic Chemistry and Materia Medica, Hubei Engineering Research Center for Biomaterials and Medical Protective Materials, School of Chemistry and Chemical Engineering, Huazhong University of Science and Technology, Wuhan 430074, China. (Email: [Lmyang@hust.edu.cn](mailto:Lmyang@hust.edu.cn))*

**Table S1.** The lattice parameters (Å), space groups and point groups of optimized crystal structures of M<sub>2</sub>Pc monolayers.

**Table S2.** Calculated elastic constants ( $C_{ij}$ , N/m), Layer modulus ( $\gamma$ , N/m), Young's modulus ( $Y$ , N/m), Poisson's ratio ( $\nu$ ) of M<sub>2</sub>Pc nanosheets.

**Table S3.** Calculated lattice parameters (Å), crystal structures for Mg<sub>2</sub>Pc monolayer under biaxial strain from -5% to 10%.

**Table S4.** Calculated lattice parameters (Å), crystal structures for Ca<sub>2</sub>Pc monolayer under biaxial strain from -5% to 10%.

**Table S5.** Calculated lattice parameters (Å), crystal structures for Sr<sub>2</sub>Pc monolayer under biaxial strain from -5% to 10%.

**Table S6.** Calculated lattice parameters (Å), crystal structures for Ba<sub>2</sub>Pc monolayer under biaxial strain from -5% to 10%.

**Table S7.** Calculated electronic band structures for Be<sub>2</sub>Pc monolayer under biaxial strain from -5% to 10%.

**Table S8.** Calculated electronic band structures for Mg<sub>2</sub>Pc monolayer under biaxial strain from -5% to 10%.

**Table S9.** Calculated electronic band structures for Ca<sub>2</sub>Pc monolayer under biaxial strain from -5% to 10%.

**Table S10.** Calculated electronic band structures for Sr<sub>2</sub>Pc monolayer under biaxial strain from -5% to 10%.

**Table S11.** Calculated electronic band structures for Ba<sub>2</sub>Pc monolayer under biaxial strain from -5% to 10%.

**Table S12.** Computed effective mass ( $m^*$ ,  $m_0$ ), deformation potential constant ( $E_1$ , eV), 2D elastic modulus ( $C_{2D}$ , N/m), and carrier mobility ( $\mu$ , cm<sup>2</sup> V<sup>-1</sup> s<sup>-1</sup>) of electrons and holes along  $x$  and  $y$  directions for the M<sub>2</sub>Pc sheets at 300 K.

**Table S13.** Calculated band gap of the donor ( $E_g$ ), conduction band offset ( $\Delta E_c$ ), open circuit voltage ( $V_{oc}$ ), the ratio of short circuit current density to AM1.5 solar energy flux ( $J_{sc}/P_{solar}$ ) and PCE of heterostructures.

**Figure S1.** Variations of temperature and energy against the time for AIMD simulations of the Be<sub>2</sub>Pc monolayer.

**Figure S2.** Variations of temperature and energy against the time for AIMD simulations of the Mg<sub>2</sub>Pc monolayer.

**Figure S3.** Variations of temperature and energy against the time for AIMD simulations of the Ca<sub>2</sub>Pc monolayer.

**Figure S4.** Variations of temperature and energy against the time for AIMD simulations of the Sr<sub>2</sub>Pc monolayer.

**Figure S5.** Variations of temperature and energy against the time for AIMD simulations of the Ba<sub>2</sub>Pc monolayer.

**Figure S6.** Calculated electronic band structures and corresponding total density of states (DOS) based for (a) Mg<sub>2</sub>Pc, (b) Ca<sub>2</sub>Pc, (c) Sr<sub>2</sub>Pc and (d) Ba<sub>2</sub>Pc monolayers at the PBE level. The Fermi level ( $E_F$ ) is set to zero and marked with the dotted line.

**Figure S7.** Calculated band structures of (a) Mg<sub>2</sub>Pc, (b) Ca<sub>2</sub>Pc, (c) Sr<sub>2</sub>Pc and (d) Ba<sub>2</sub>Pc monolayers at the HSE06 level. The Fermi level is set at 0 eV.

**Figure S8.** The partial charge density distribution of the CBM (blue) and VBM (red) for the M<sub>2</sub>Pc monolayers. The isosurface value is 0.003 e/Bohr<sup>3</sup>.

**Figure S9.** Calculated PDOS of the 2D M<sub>2</sub>Pc monolayers in the range of -1.5 to 1.5 eV. Rows represent the PDOS contributions from different types of atoms. The last row shows TDOS for each material.

**Figure S10.** The evolution of PDOS on different atoms near the Fermi level versus biaxial strain from -5% to 10% for Be<sub>2</sub>Pc monolayer. The Fermi level has been set to 0 eV.

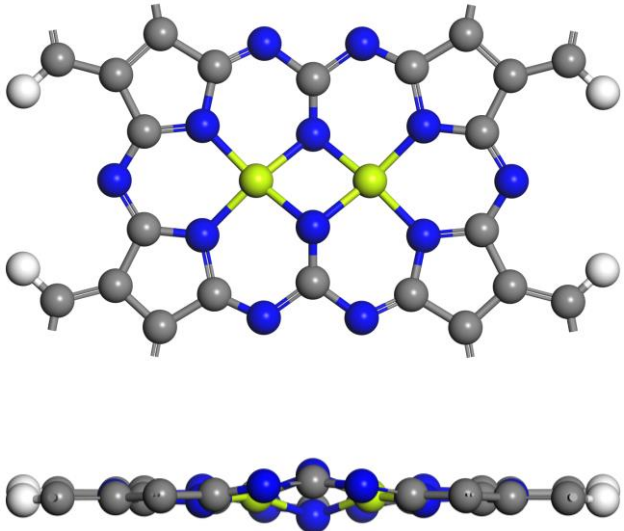
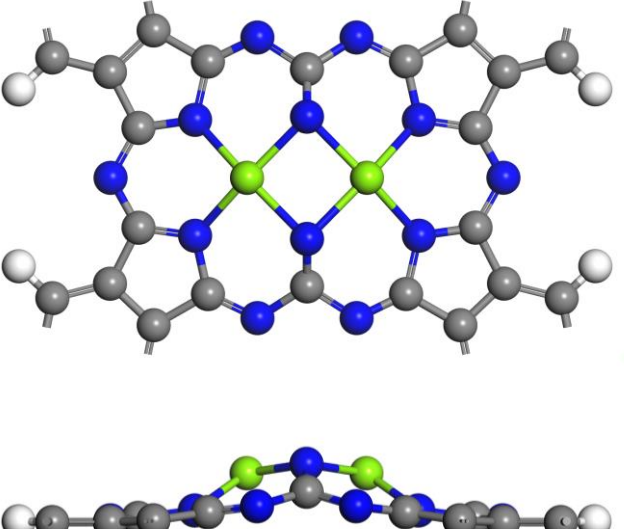
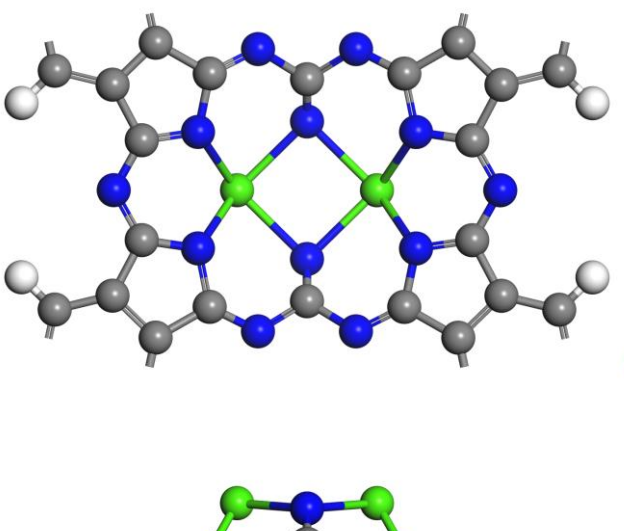
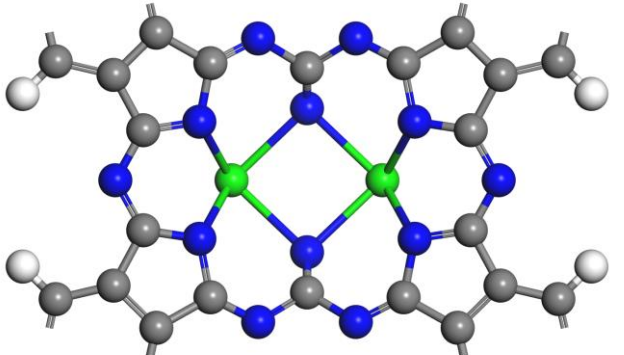
**Figure S11.** The evolution of PDOS on different atoms near the Fermi level versus biaxial strain from -5% to 10% for Mg<sub>2</sub>Pc monolayer. The Fermi level has been set to 0 eV.

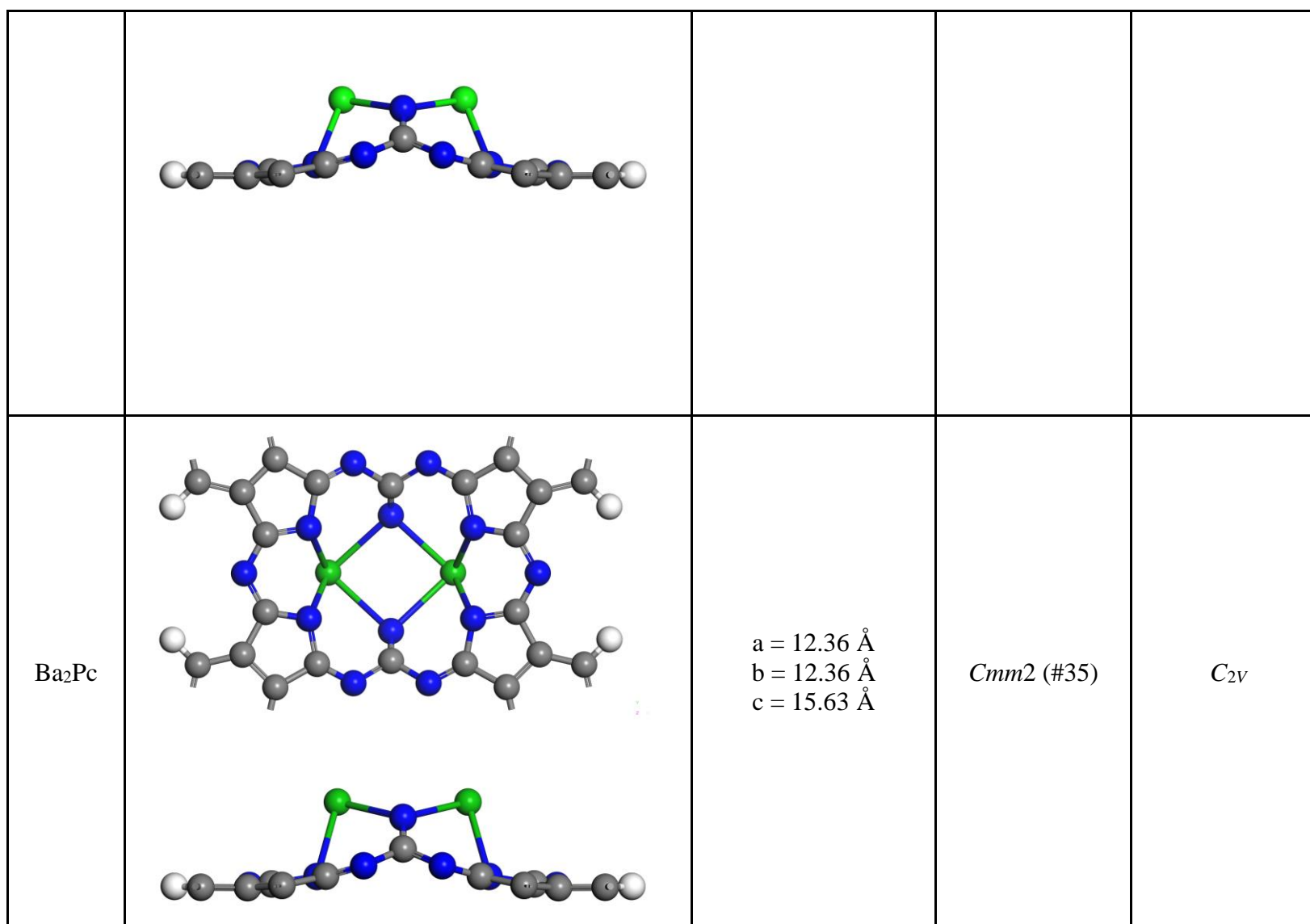
**Figure S12.** The evolution of PDOS on different atoms near the Fermi level versus biaxial strain from -5% to 10% for Ca<sub>2</sub>Pc monolayer. The Fermi level has been set to 0 eV.

**Figure S13.** The evolution of PDOS on different atoms near the Fermi level versus biaxial strain from -5% to 10% for Sr<sub>2</sub>Pc monolayer. The Fermi level has been set to 0 eV.

**Figure S14.** The evolution of PDOS on different atoms near the Fermi level versus biaxial strain from -5% to 10% for Ba<sub>2</sub>Pc monolayer. The Fermi level has been set to 0 eV.

**Table S1.** The lattice parameters ( $\text{\AA}$ ), space groups and point groups of optimized crystal structures of  $M_2Pc$  monolayers.

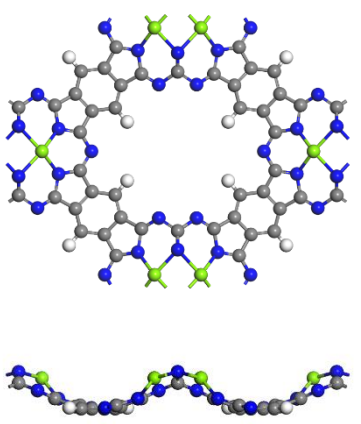
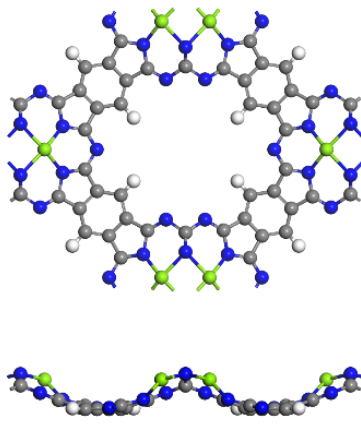
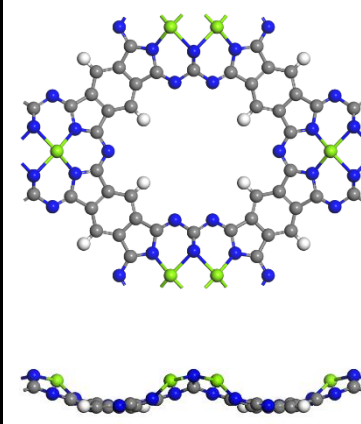
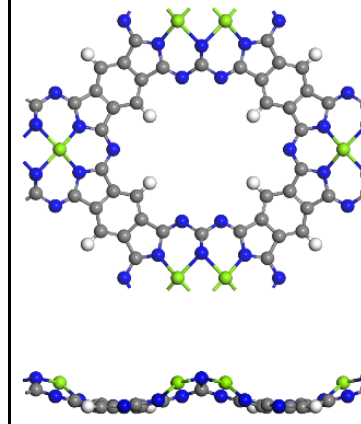
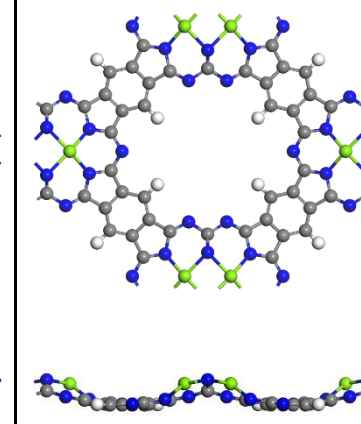
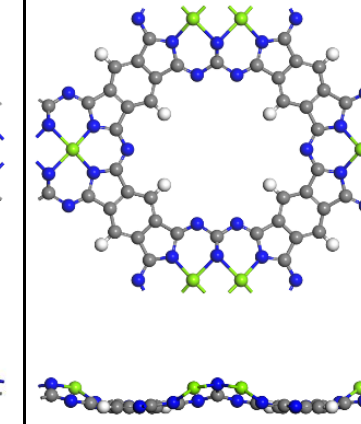
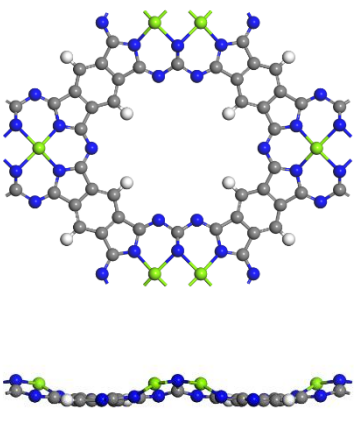
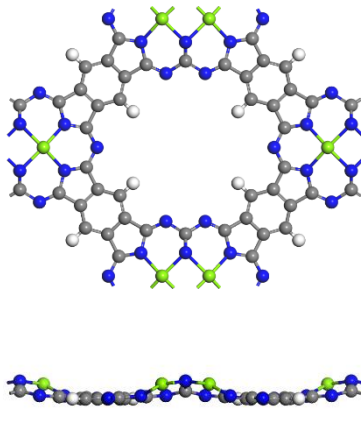
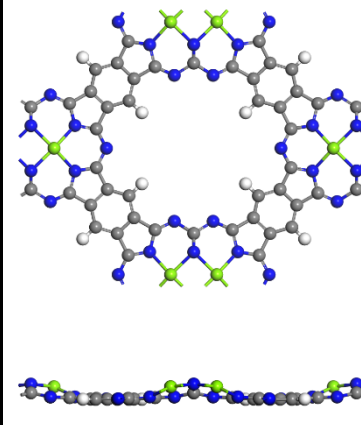
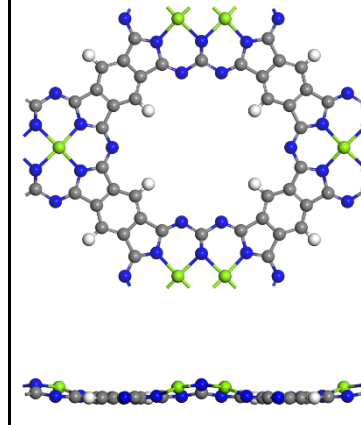
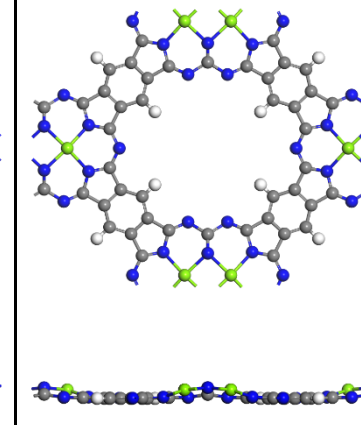
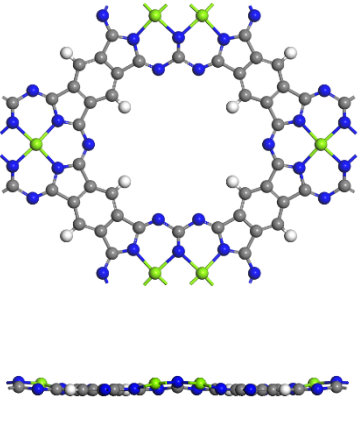
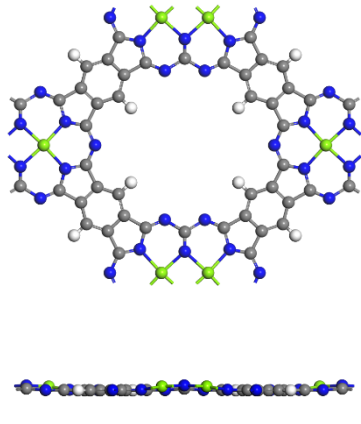
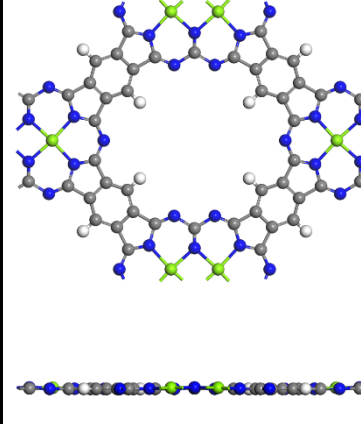
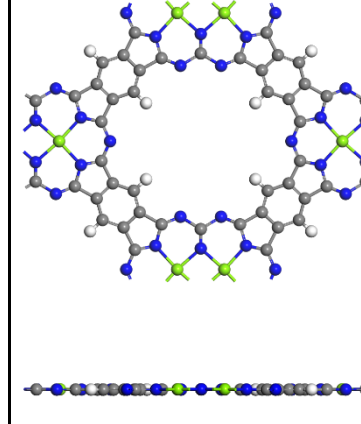
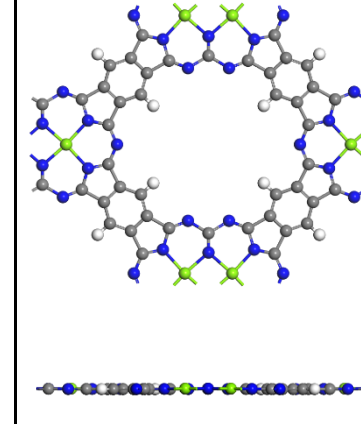
$M_2Pc$	Optimized structure top (up) and side (down) views	Lattice constant	Space group	Point group
$Be_2Pc$		$a = 12.34 \text{ \AA}$ $b = 12.34 \text{ \AA}$ $c = 15.09 \text{ \AA}$	$C2/m$ (#12)	$C_{2h}$
$Mg_2Pc$		$a = 12.48 \text{ \AA}$ $b = 12.48 \text{ \AA}$ $c = 15.36 \text{ \AA}$	$Cmm2$ (#35)	$C_{2v}$
$Ca_2Pc$		$a = 12.40 \text{ \AA}$ $b = 12.40 \text{ \AA}$ $c = 15.53 \text{ \AA}$	$Cmm2$ (#35)	$C_{2v}$
$Sr_2Pc$		$a = 12.38 \text{ \AA}$ $b = 12.38 \text{ \AA}$ $c = 15.58 \text{ \AA}$	$Cmm2$ (#35)	$C_{2v}$



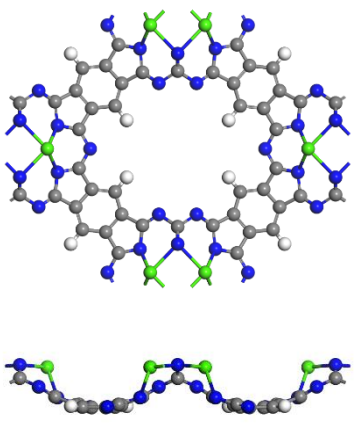
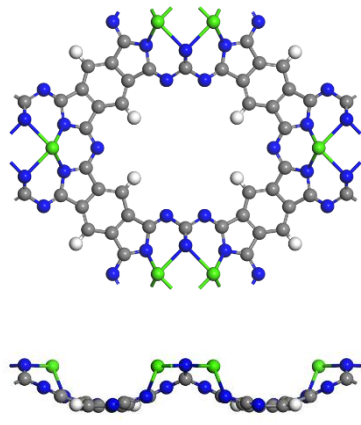
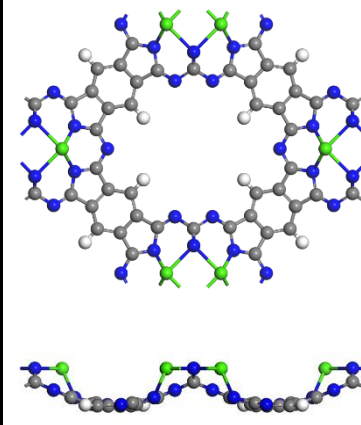
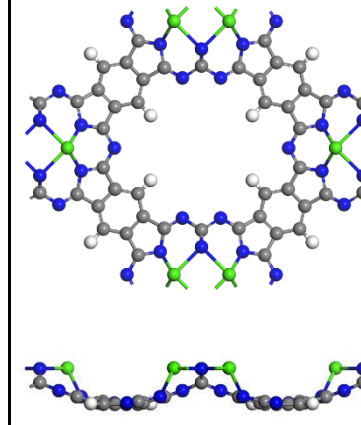
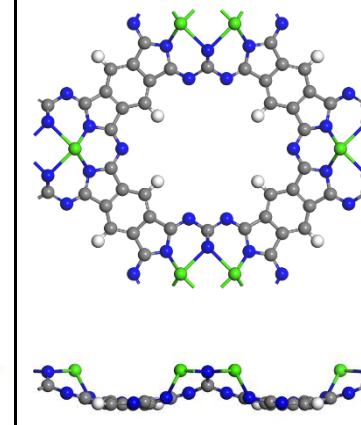
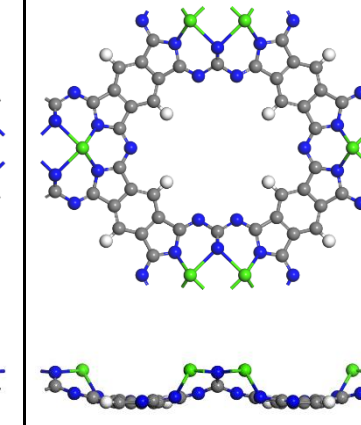
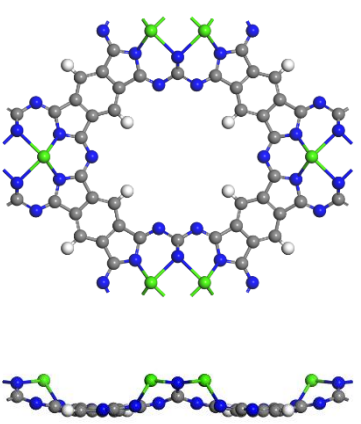
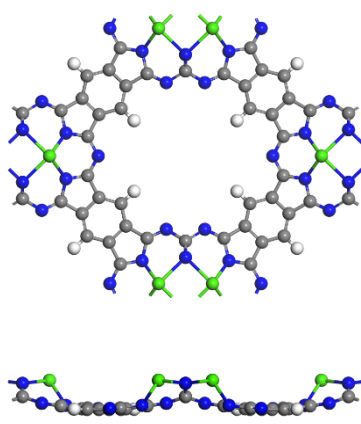
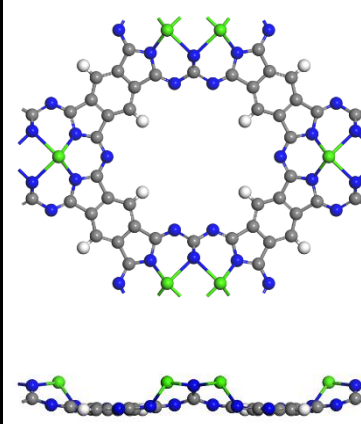
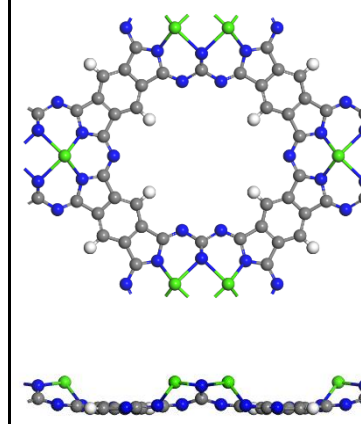
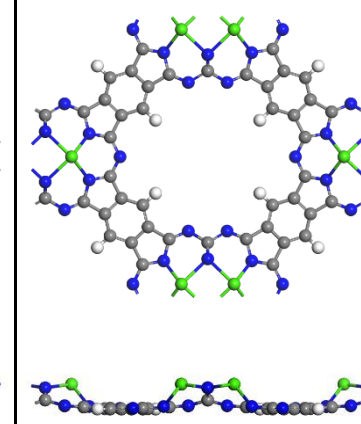
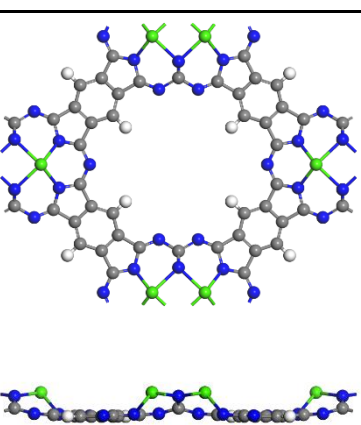
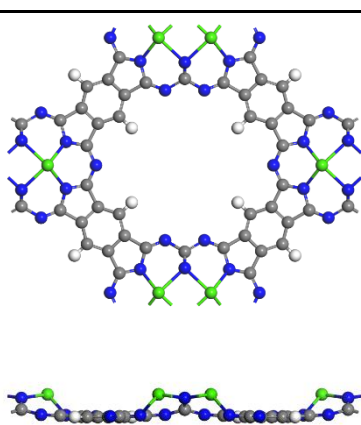
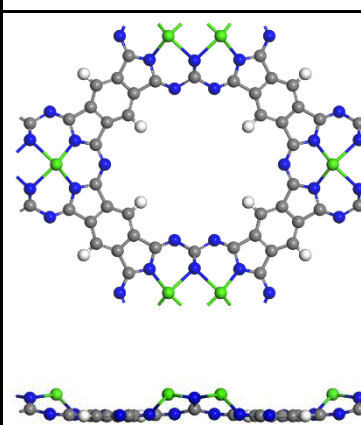
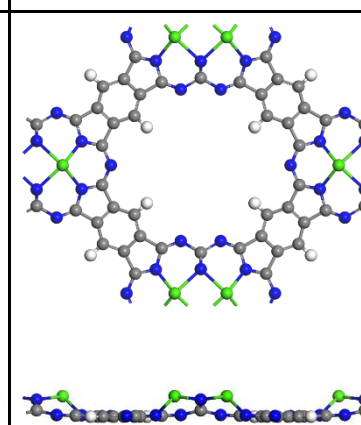
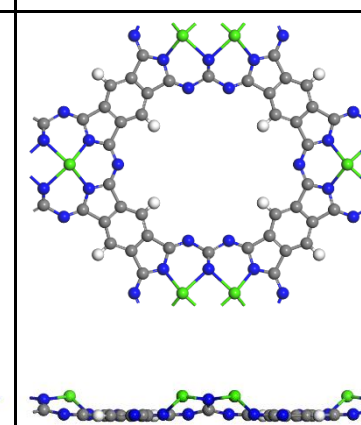
**Table S2.** Calculated elastic constants ( $C_{ij}$ , N/m), Layer modulus ( $\gamma$ , N/m), Young's modulus ( $Y$ , N/m), Poisson's ratio ( $\nu$ ) of  $M_2Pc$  nanosheets.

Structure	$C_{11}$	$C_{22}$	$C_{12}$	$C_{66}$	$\gamma$	Young modulus		Poisson's ratio	
						$Y_x$	$Y_y$	$\nu_x$	$\nu_y$
Be <sub>2</sub> Pc	71.7	70.2	24.0	18.4	47.5	63.5	62.1	0.34	0.33
Mg <sub>2</sub> Pc	57.3	56.4	21.6	16.9	39.2	49.1	48.2	0.38	0.38
Ca <sub>2</sub> Pc	44.2	44.4	22.2	15.3	33.2	33.1	33.3	0.50	0.50
Sr <sub>2</sub> Pc	40.6	41.1	21.1	14.7	30.9	29.8	30.1	0.51	0.52
Ba <sub>2</sub> Pc	38.1	38.7	20.4	14.3	29.4	27.3	27.8	0.53	0.54

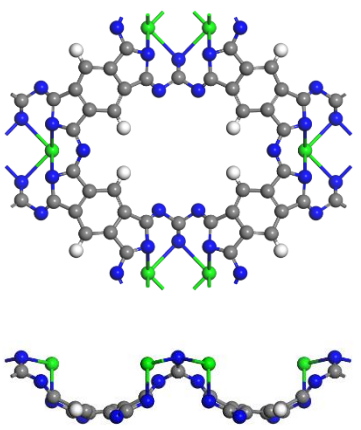
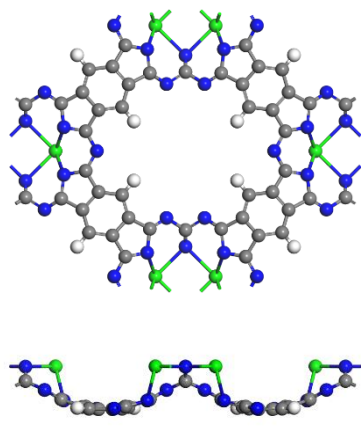
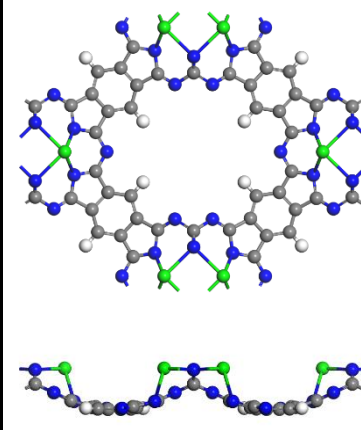
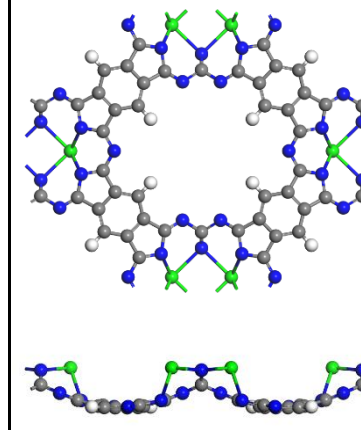
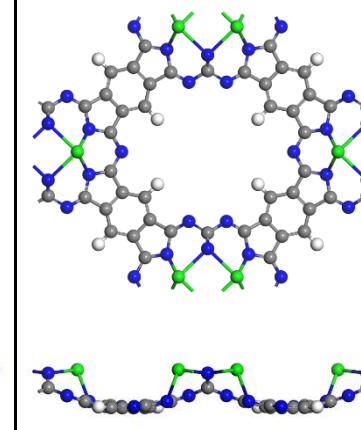
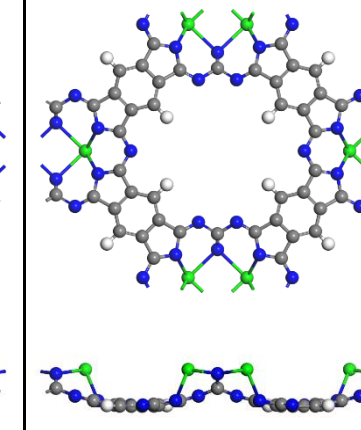
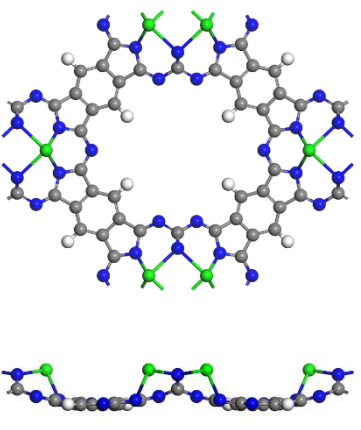
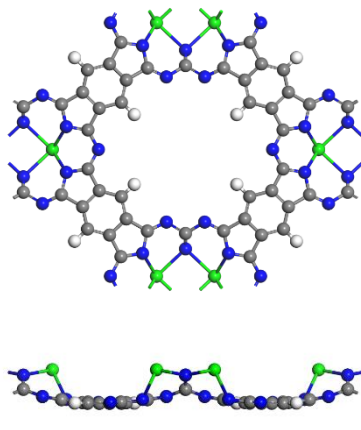
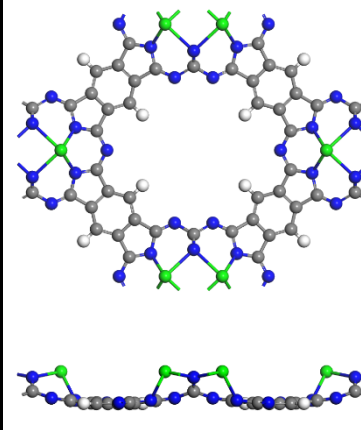
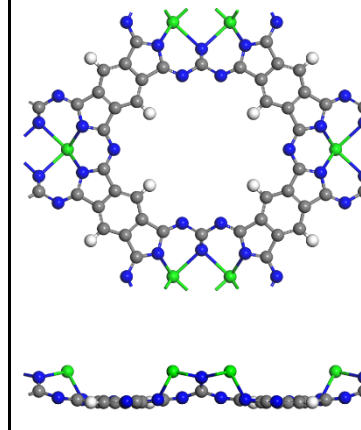
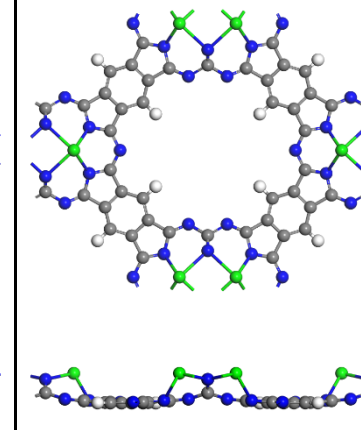
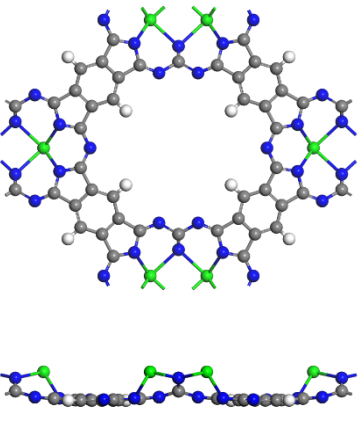
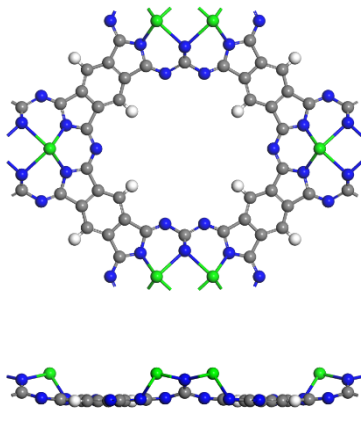
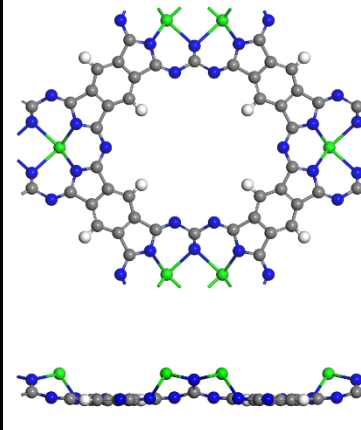
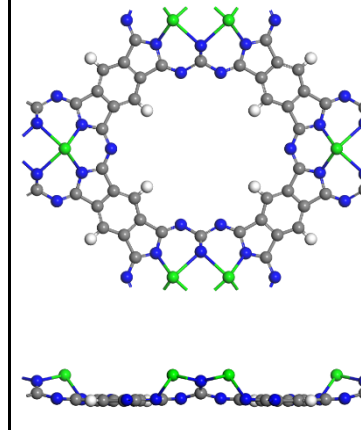
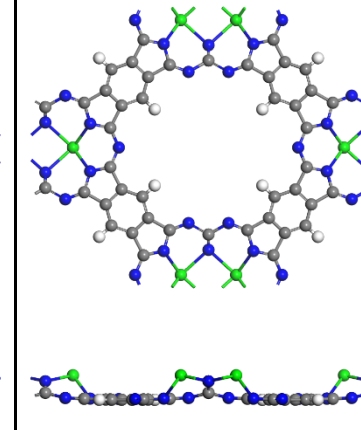
**Table S3.** Calculated lattice parameters (Å), crystal structures for Mg<sub>2</sub>Pc monolayer under biaxial strain from -5% to 10%.

Strain	-5%	-4%	-3%	-2%	-1%	0%
Lattice constant	a = 14.54 Å b = 18.74 Å c = 15.36 Å	a = 14.69 Å b = 18.93 Å c = 15.36 Å	a = 14.85 Å b = 19.13 Å c = 15.36 Å	a = 15.00 Å b = 19.33 Å c = 15.36 Å	a = 15.15 Å b = 19.52 Å c = 15.36 Å	a = 15.31 Å b = 19.72 Å c = 15.36 Å
Mg <sub>2</sub> Pc						
Strain	1%	2%	3%	4%	5%	
Lattice constant	a = 15.46 Å b = 19.92 Å c = 15.36 Å	a = 15.61 Å b = 20.12 Å c = 15.36 Å	a = 15.76 Å b = 20.31 Å c = 15.36 Å	a = 15.92 Å b = 20.51 Å c = 15.36 Å	a = 16.07 Å b = 20.70 Å c = 15.36 Å	
Mg <sub>2</sub> Pc						
Strain	6%	7%	8%	9%	10%	
Lattice constant	a = 16.22 Å b = 20.90 Å c = 15.36 Å	a = 16.38 Å b = 21.10 Å c = 15.36 Å	a = 16.53 Å b = 21.30 Å c = 15.36 Å	a = 16.68 Å b = 21.50 Å c = 15.36 Å	a = 13.77 Å b = 17.75 Å c = 15.36 Å	
Mg <sub>2</sub> Pc						

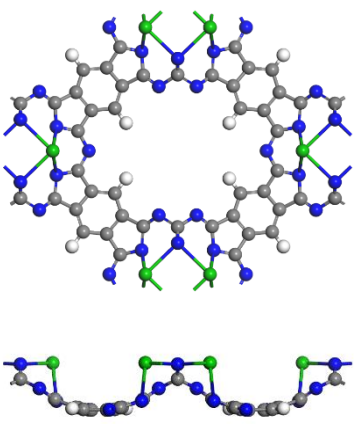
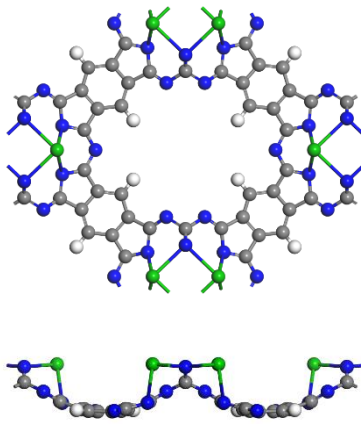
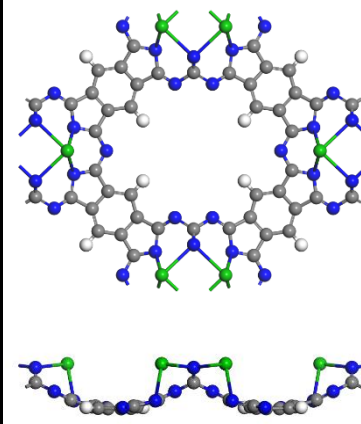
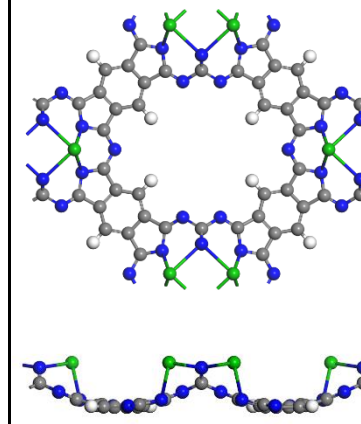
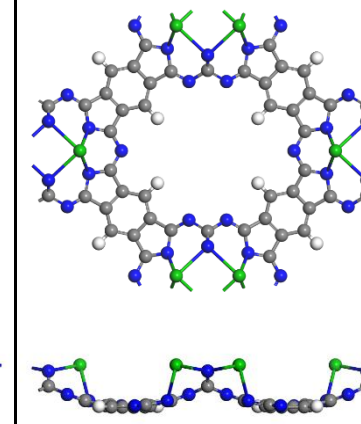
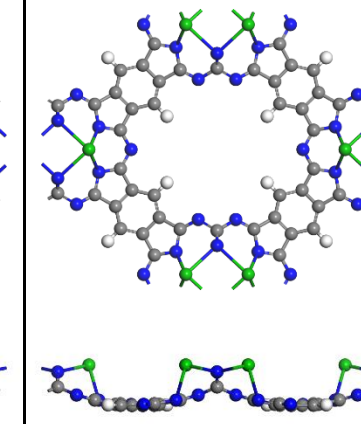
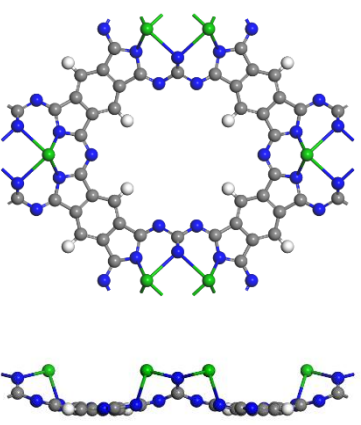
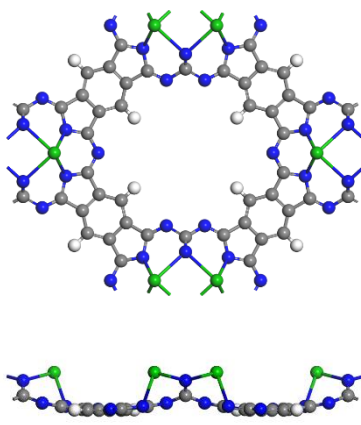
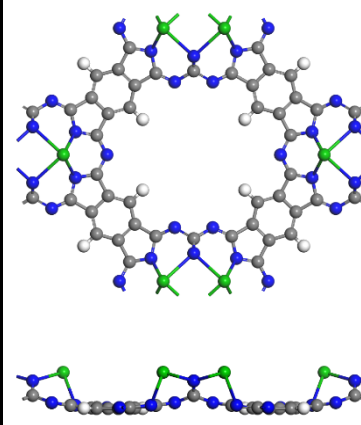
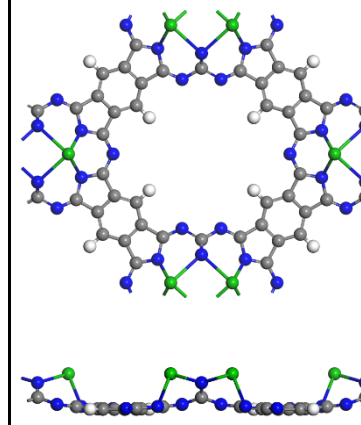
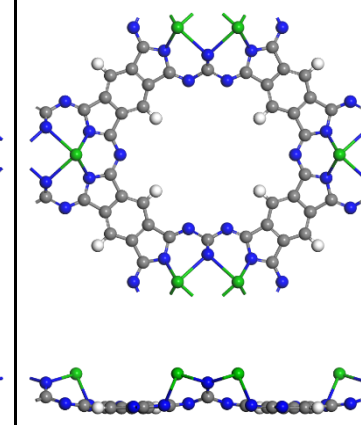
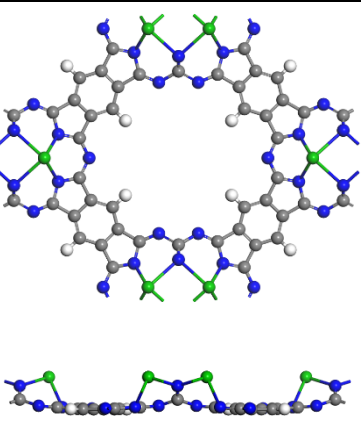
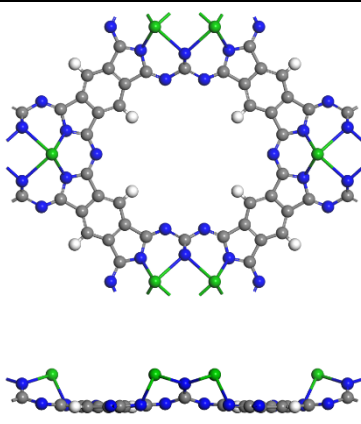
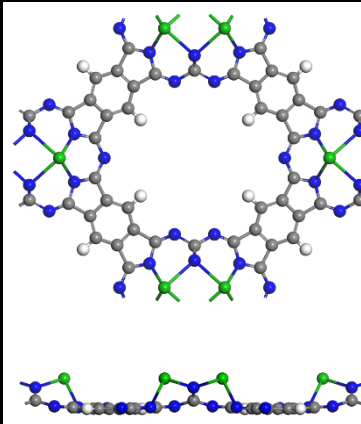
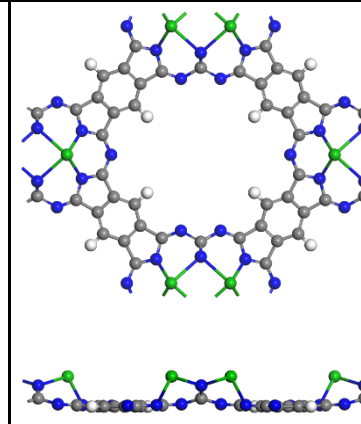
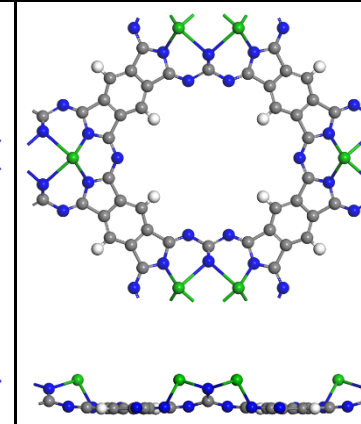
**Table S4.** Calculated lattice parameters (Å), crystal structures for Ca<sub>2</sub>Pc monolayer under biaxial strain from -5% to 10%.

Strain	-5%	-4%	-3%	-2%	-1%	0%
Lattice constant	a = 14.50 Å b = 18.57 Å c = 15.54 Å	a = 14.65 Å b = 18.77 Å c = 15.54 Å	a = 14.81 Å b = 18.97 Å c = 15.54 Å	a = 14.96 Å b = 19.16 Å c = 15.54 Å	a = 15.11 Å b = 19.36 Å c = 15.54 Å	a = 15.26 Å b = 19.55 Å c = 15.54 Å
Ca <sub>2</sub> Pc						
Strain	1%	2%	3%	4%	5%	
Lattice constant	a = 15.42 Å b = 19.75 Å c = 15.54 Å	a = 15.57 Å b = 19.95 Å c = 15.54 Å	a = 15.72 Å b = 20.14 Å c = 15.54 Å	a = 15.87 Å b = 20.33 Å c = 15.54 Å	a = 16.03 Å b = 20.53 Å c = 15.54 Å	
Ca <sub>2</sub> Pc						
Strain	6%	7%	8%	9%	10%	
Lattice constant	a = 16.18 Å b = 20.72 Å c = 15.54 Å	a = 16.33 Å b = 20.92 Å c = 15.54 Å	a = 16.49 Å b = 21.12 Å c = 15.54 Å	a = 16.64 Å b = 21.31 Å c = 15.54 Å	a = 16.791 Å b = 21.51 Å c = 15.54 Å	
Ca <sub>2</sub> Pc						

**Table S5.** Calculated lattice parameters ( $\text{\AA}$ ), crystal structures for  $\text{Sr}_2\text{Pc}$  monolayer under biaxial strain from  $-5\%$  to  $10\%$ .

Strain	$-5\%$	$-4\%$	$-3\%$	$-2\%$	$-1\%$	$0\%$
Lattice constant	$a = 14.49 \text{ \AA}$ $b = 18.54 \text{ \AA}$ $c = 15.58 \text{ \AA}$	$a = 14.64 \text{ \AA}$ $b = 18.73 \text{ \AA}$ $c = 15.58 \text{ \AA}$	$a = 14.79 \text{ \AA}$ $b = 18.93 \text{ \AA}$ $c = 15.63 \text{ \AA}$	$a = 14.945 \text{ \AA}$ $b = 19.125 \text{ \AA}$ $c = 15.58 \text{ \AA}$	$a = 15.10 \text{ \AA}$ $b = 19.32 \text{ \AA}$ $c = 15.63 \text{ \AA}$	$a = 15.25 \text{ \AA}$ $b = 19.52 \text{ \AA}$ $c = 15.58 \text{ \AA}$
$\text{Sr}_2\text{Pc}$						
Strain	$1\%$	$2\%$	$3\%$	$4\%$	$5\%$	
Lattice constant	$a = 15.40 \text{ \AA}$ $b = 19.71 \text{ \AA}$ $c = 15.58 \text{ \AA}$	$a = 15.55 \text{ \AA}$ $b = 19.90 \text{ \AA}$ $c = 15.58 \text{ \AA}$	$a = 15.71 \text{ \AA}$ $b = 20.10 \text{ \AA}$ $c = 15.58 \text{ \AA}$	$a = 15.86 \text{ \AA}$ $b = 20.29 \text{ \AA}$ $c = 15.58 \text{ \AA}$	$a = 16.01 \text{ \AA}$ $b = 20.49 \text{ \AA}$ $c = 15.58 \text{ \AA}$	
$\text{Sr}_2\text{Pc}$						
Strain	$6\%$	$7\%$	$8\%$	$9\%$	$10\%$	
Lattice constant	$a = 16.17 \text{ \AA}$ $b = 20.69 \text{ \AA}$ $c = 15.58 \text{ \AA}$	$a = 16.32 \text{ \AA}$ $b = 20.88 \text{ \AA}$ $c = 15.58 \text{ \AA}$	$a = 16.47 \text{ \AA}$ $b = 21.08 \text{ \AA}$ $c = 15.58 \text{ \AA}$	$a = 16.62 \text{ \AA}$ $b = 21.27 \text{ \AA}$ $c = 15.58 \text{ \AA}$	$a = 16.77 \text{ \AA}$ $b = 21.46 \text{ \AA}$ $c = 15.58 \text{ \AA}$	
$\text{Sr}_2\text{Pc}$						

**Table S6.** Calculated lattice parameters (Å), crystal structures for Ba<sub>2</sub>Pc monolayer under biaxial strain from -5% to 10%.

Strain	-5%	-4%	-3%	-2%	-1%	0%
Lattice constant	a = 14.48 Å b = 18.49 Å c = 15.63 Å	a = 14.63 Å b = 18.69 Å c = 15.63 Å	a = 14.78 Å b = 18.88 Å c = 15.63 Å	a = 14.93 Å b = 19.08 Å c = 15.63 Å	a = 15.09 Å b = 19.27 Å c = 15.63 Å	a = 15.24 Å b = 19.47 Å c = 15.63 Å
Ba <sub>2</sub> Pc						
Strain	1%	2%	3%	4%	5%	
Lattice constant	a = 15.39 Å b = 19.66 Å c = 15.63 Å	a = 15.54 Å b = 19.85 Å c = 15.63 Å	a = 15.70 Å b = 20.05 Å c = 15.63 Å	a = 15.85 Å b = 20.24 Å c = 15.63 Å	a = 16.00 Å b = 20.44 Å c = 15.63 Å	
Ba <sub>2</sub> Pc						
Strain	6%	7%	8%	9%	10%	
Lattice constant	a = 16.15 Å b = 20.63 Å c = 15.63 Å	a = 16.31 Å b = 20.83 Å c = 15.63 Å	a = 16.46 Å b = 21.02 Å c = 15.63 Å	a = 16.61 Å b = 21.22 Å c = 15.63 Å	a = 16.76 Å b = 21.41 Å c = 15.63 Å	
Ba <sub>2</sub> Pc						

**Table S7.** Calculated electronic band structures for Be<sub>2</sub>Pc monolayer under biaxial strain from -5% to 10%.

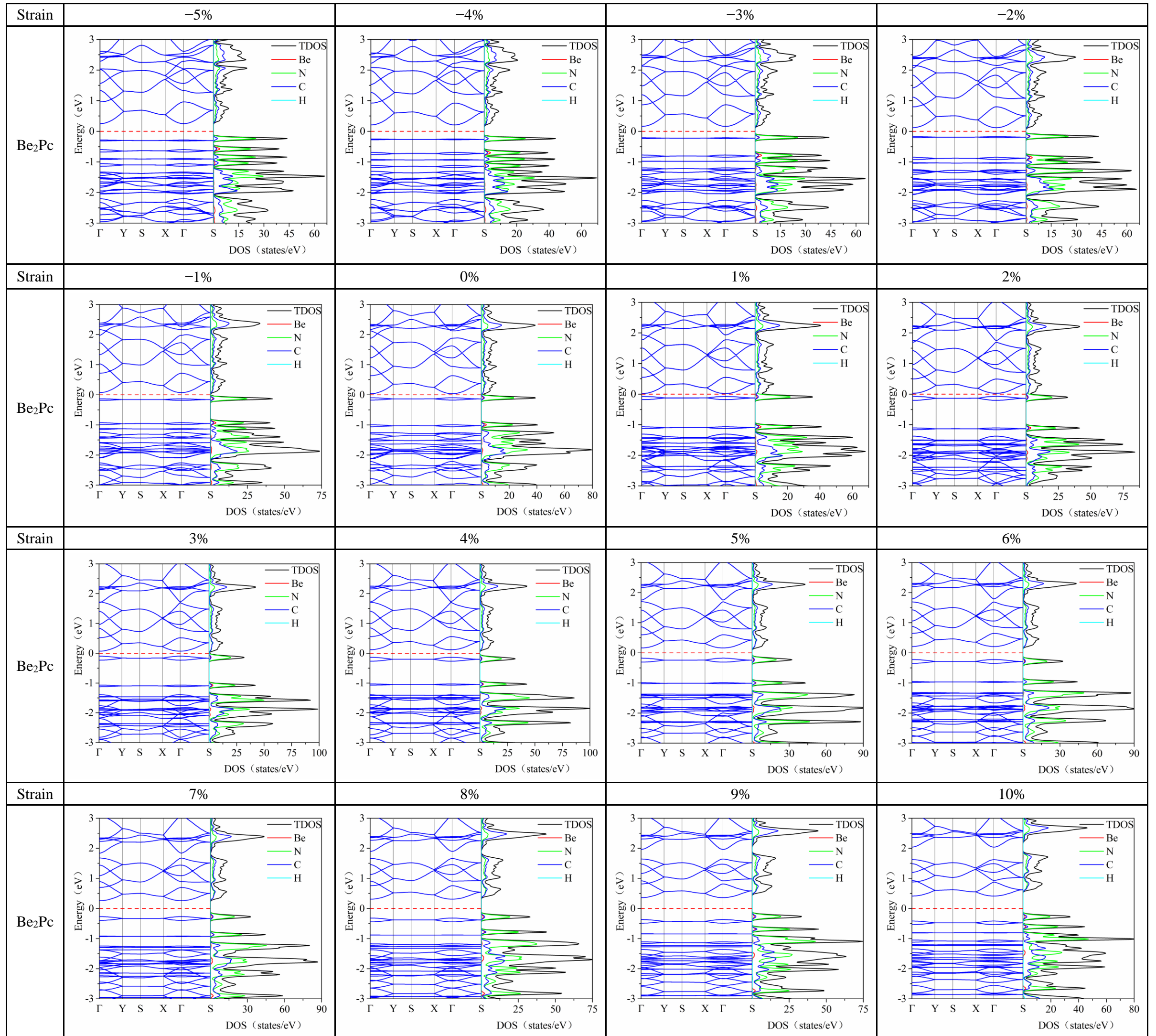




**Table S8.** Calculated electronic band structures for Mg<sub>2</sub>Pc monolayer under biaxial strain from -5% to 10%.

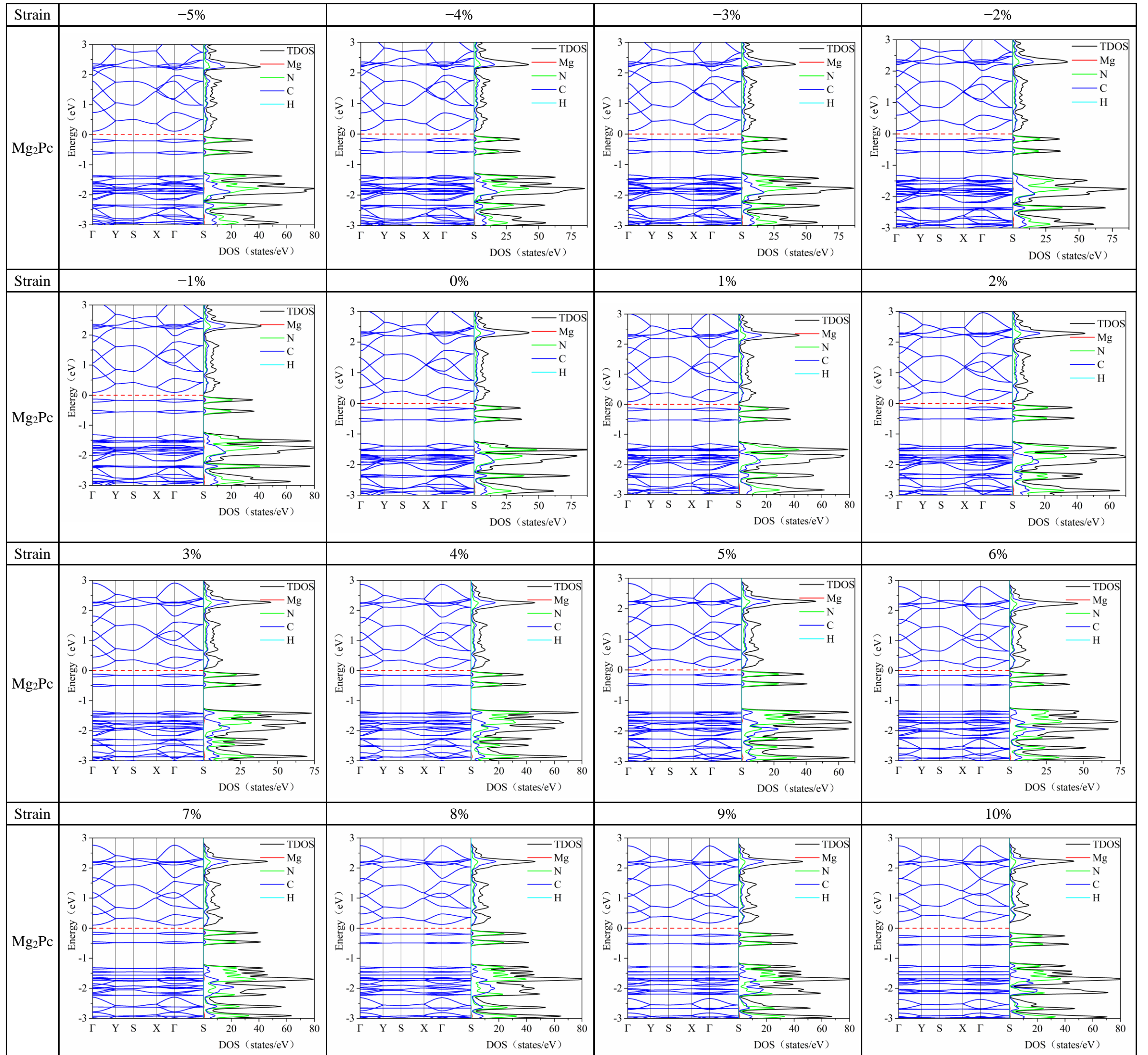


**Table S9.** Calculated electronic band structures for  $\text{Ca}_2\text{Pc}$  monolayer under biaxial strain from  $-5\%$  to  $10\%$ .

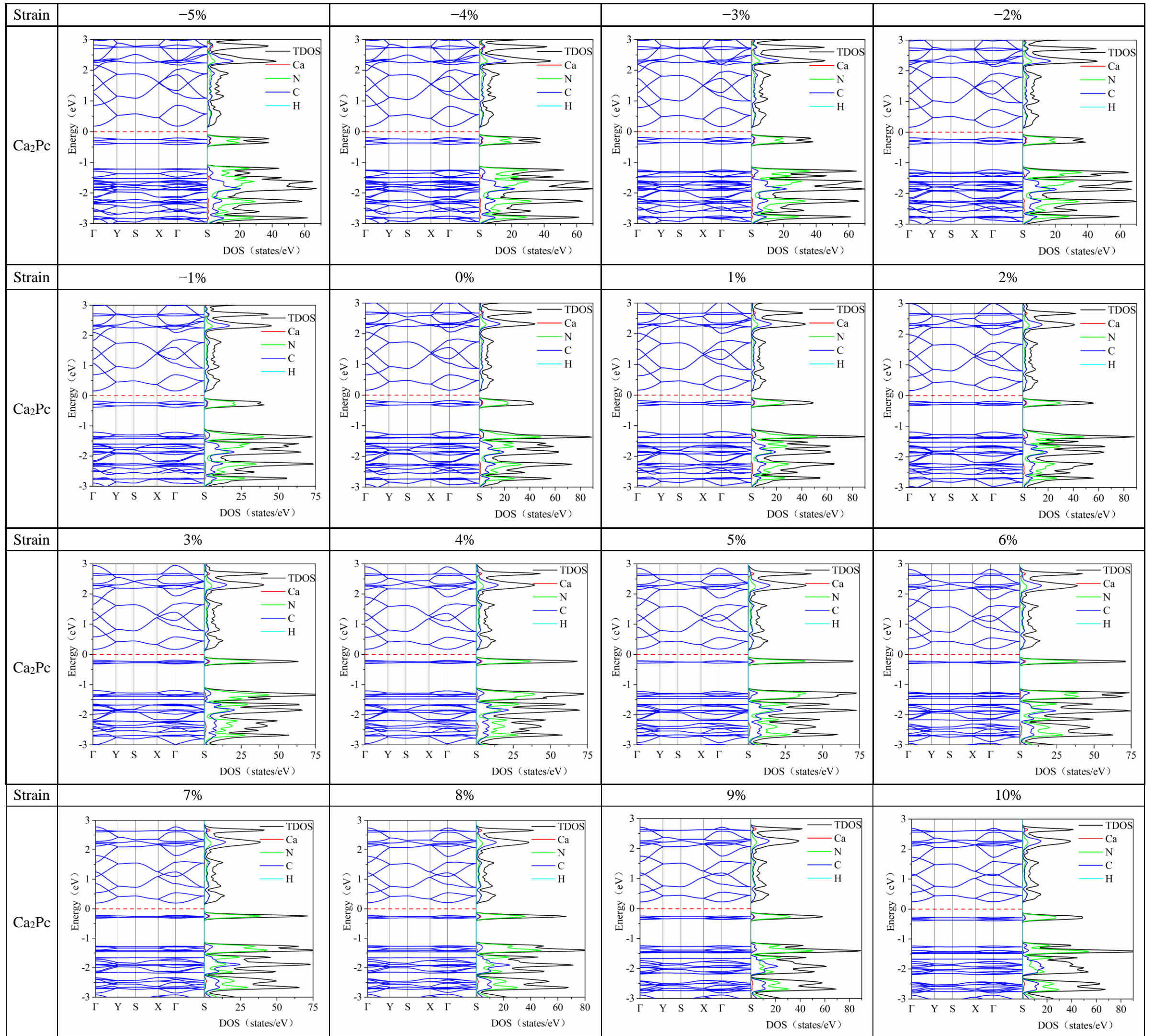


**Table S10.** Calculated electronic band structures for Sr<sub>2</sub>Pc monolayer under biaxial strain from -5% to 10%.

**Table S11.** Calculated electronic band structures for Ba<sub>2</sub>Pc monolayer under biaxial strain from -5% to 10%.

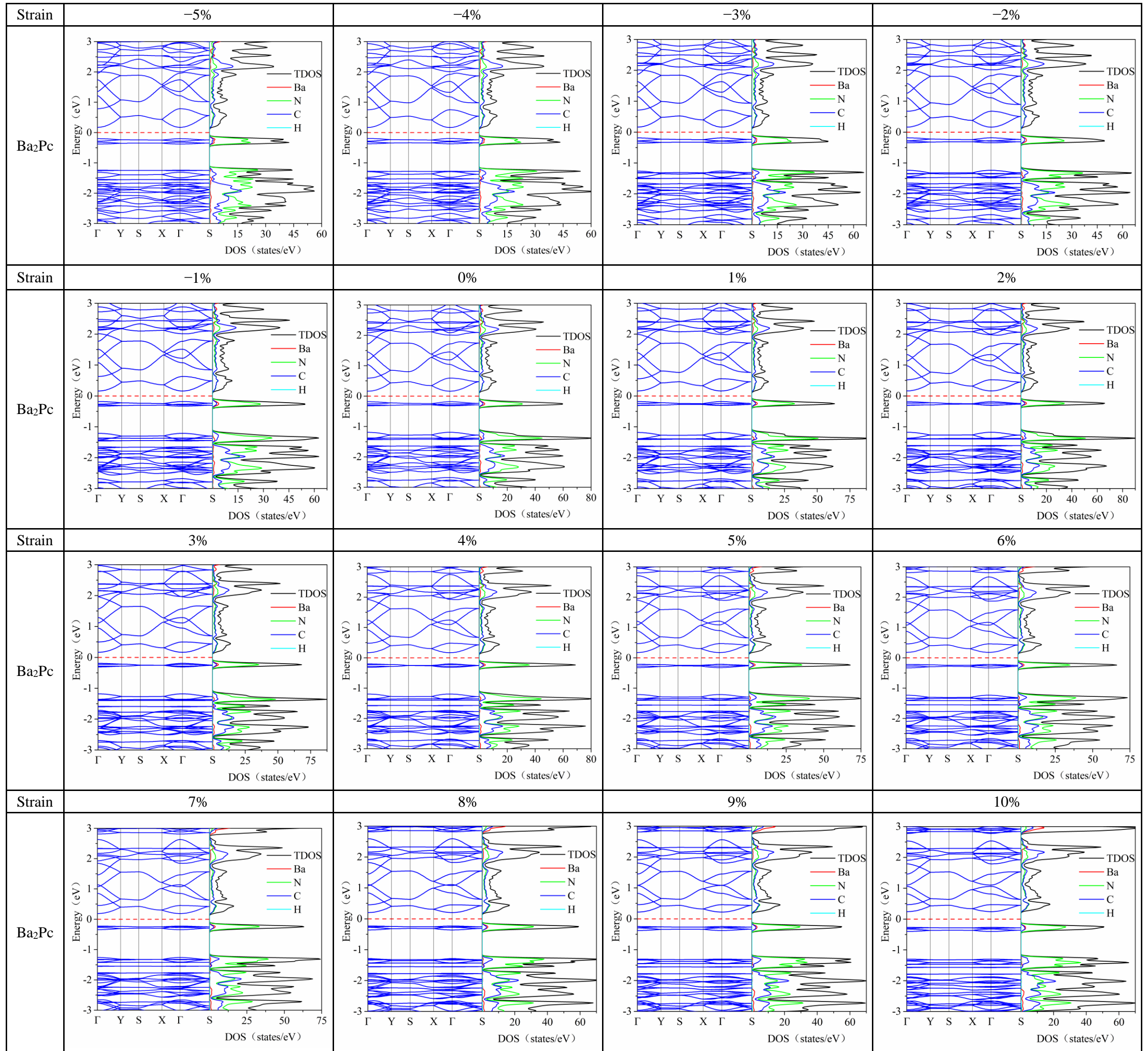


**Table S12.** Computed effective mass ( $m^*$ ,  $m_0$ ), deformation potential constant ( $E_1$ , eV), 2D elastic modulus ( $C_{2D}$ , N/m), and carrier mobility ( $\mu$ ,  $\text{cm}^2 \text{V}^{-1} \text{s}^{-1}$ ) of electrons and holes along  $x$  and  $y$  directions for the  $M_2\text{Pc}$  sheets at 300 K.

Structure	carrier type	$m_x^*$	$m_y^*$	$E_{1x}$	$E_{1y}$	$C_{2D-x}$	$C_{2D-y}$	$\mu_x$	$\mu_y$
Be <sub>2</sub> Pc	electron	0.49	0.45	0.52	0.58	64.92	61.24	19782.18	20597.23
	hole	4.02	2.59	4.59	1.20	64.92	61.24	8.95	23.61
Mg <sub>2</sub> Pc	electron	0.57	0.57	1.98	1.63	54.59	56.55	1174.43	1079.76
	hole	3.17	1.65	1.41	1.59	54.59	56.55	70.27	144.36
Ca <sub>2</sub> Pc	electron	0.55	0.44	3.54	1.61	49.45	47.65	682.49	579.20
	hole	3.69	1.37	1.70	1.97	49.45	47.65	35.95	103.12
Sr <sub>2</sub> Pc	electron	0.56	0.45	1.91	1.55	47.19	44.94	1227.48	1369.72
	hole	3.17	1.21	1.64	1.89	47.19	44.94	49.51	137.94
Ba <sub>2</sub> Pc	electron	0.57	0.48	1.91	1.56	45.58	43.04	1110.55	1193.05
	hole	3.46	1.20	1.55	2.07	45.58	43.04	38.15	125.31

**Table S13.** Calculated band gap of the donor ( $E_g$ ), conduction band offset ( $\Delta E_c$ ), open circuit voltage ( $V_{oc}$ ), the ratio of short circuit current density to AM1.5 solar energy flux ( $J_{sc}/P_{solar}$ ), and PCE of heterostructures.

Heterostructure (donor/acceptor)	$E_g$ (eV)	$\Delta E_c$ (eV)	$V_{oc}$ (eV)	$J_{sc}/P_{solar}$	$\eta$
Be <sub>2</sub> Pc/2H–MoSe <sub>2</sub>	1.21	0.05	0.86	0.422	23.61%
Mg <sub>2</sub> Pc/2H–MoTe <sub>2</sub>	1.35	0.24	0.81	0.388	20.44%
Ca <sub>2</sub> Pc/2H–WTe <sub>2</sub>	1.39	0.36	0.73	0.378	17.91%
Sr <sub>2</sub> Pc/GaN	1.35	0.14	0.91	0.389	22.88%
Ba <sub>2</sub> Pc/GaN	1.34	0.31	0.73	0.390	18.42%

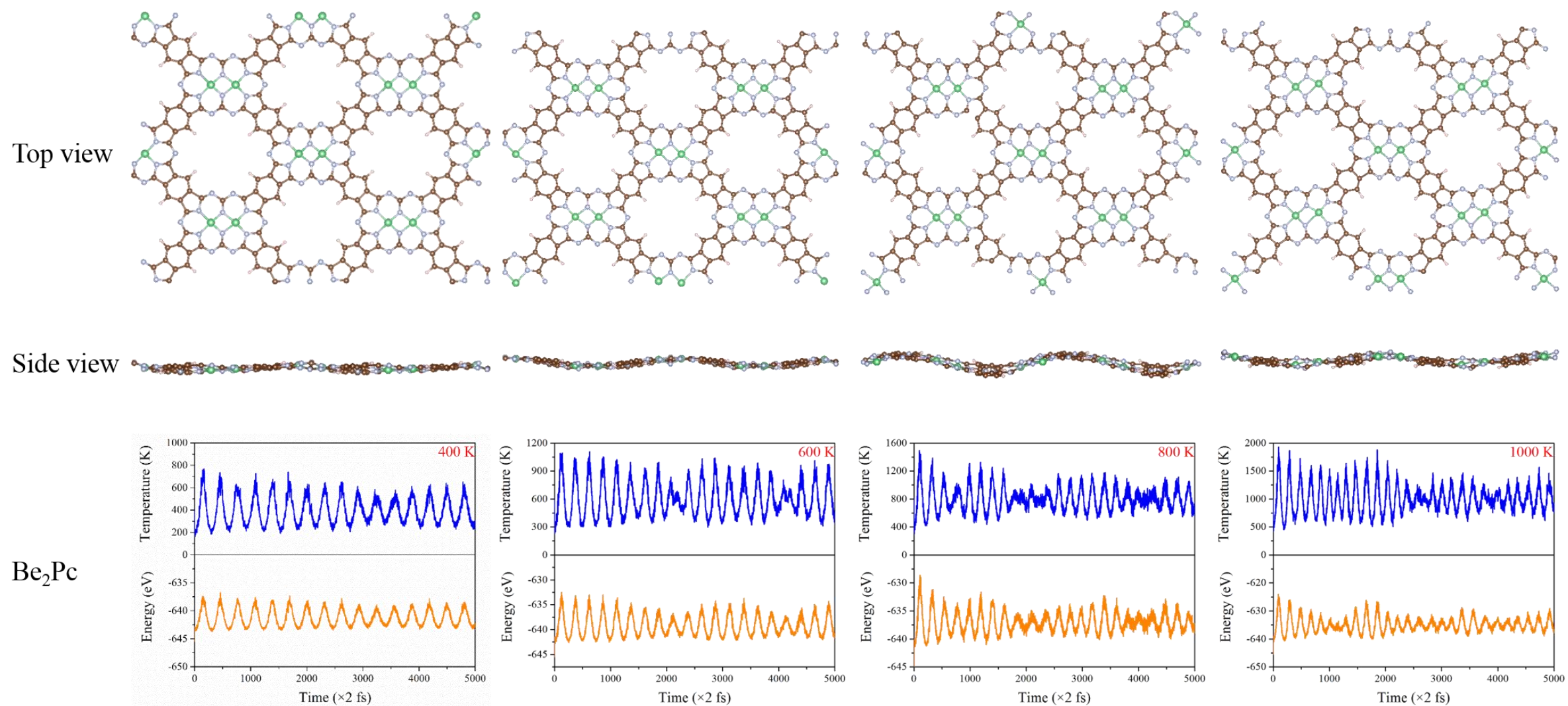


**Figure S1.** AIMD simulations results (include the final snapshot, the evolution of total energy and temperature versus the simulation time) for the Be<sub>2</sub>Pc monolayers at 400, 600, 800 and 1000 K, respectively.

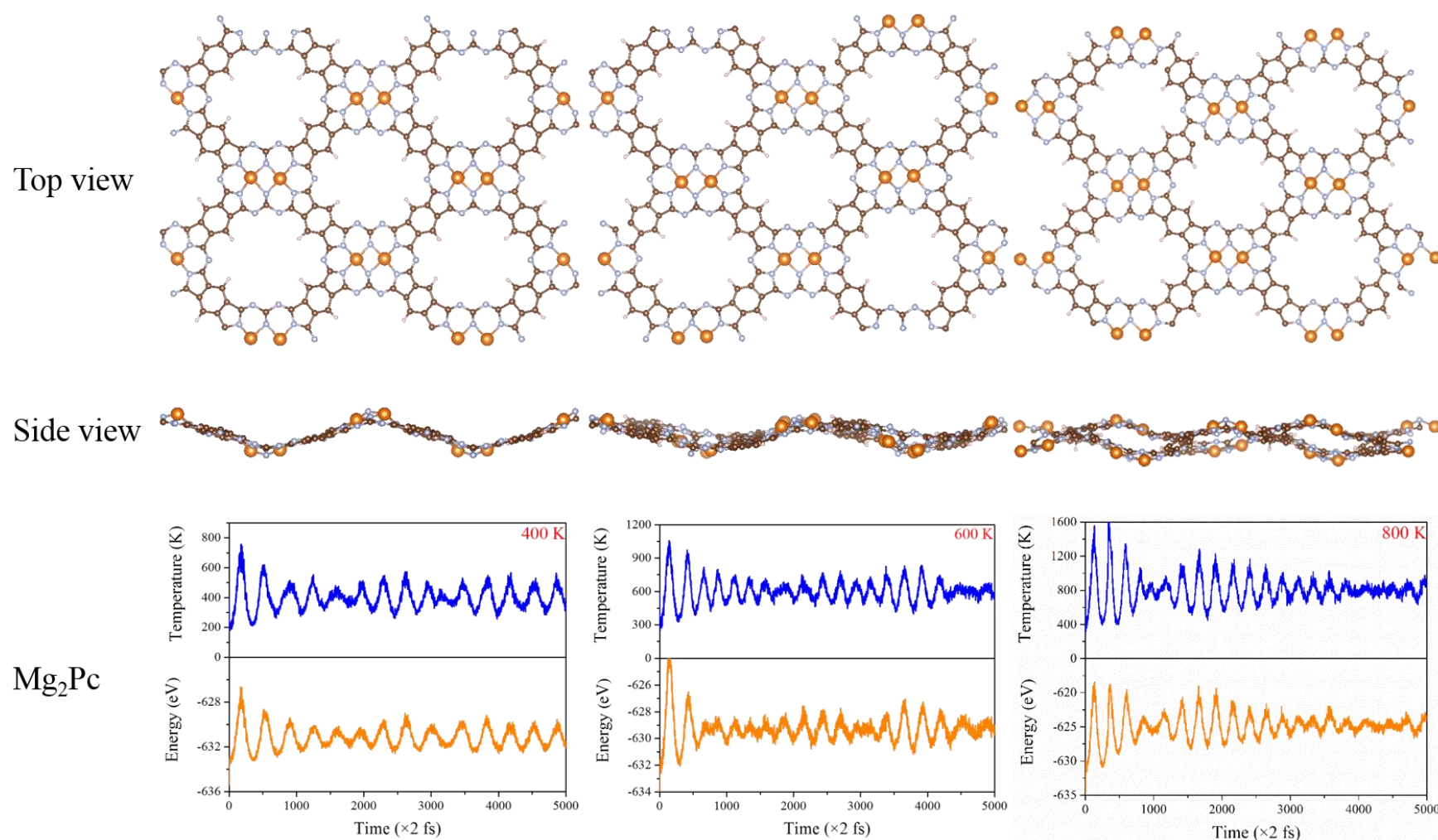


**Figure S2.** AIMD simulations results (include the final snapshot, the evolution of total energy and temperature versus the simulation time) for the Mg<sub>2</sub>Pc monolayers at 400, 600 and 800 K, respectively.

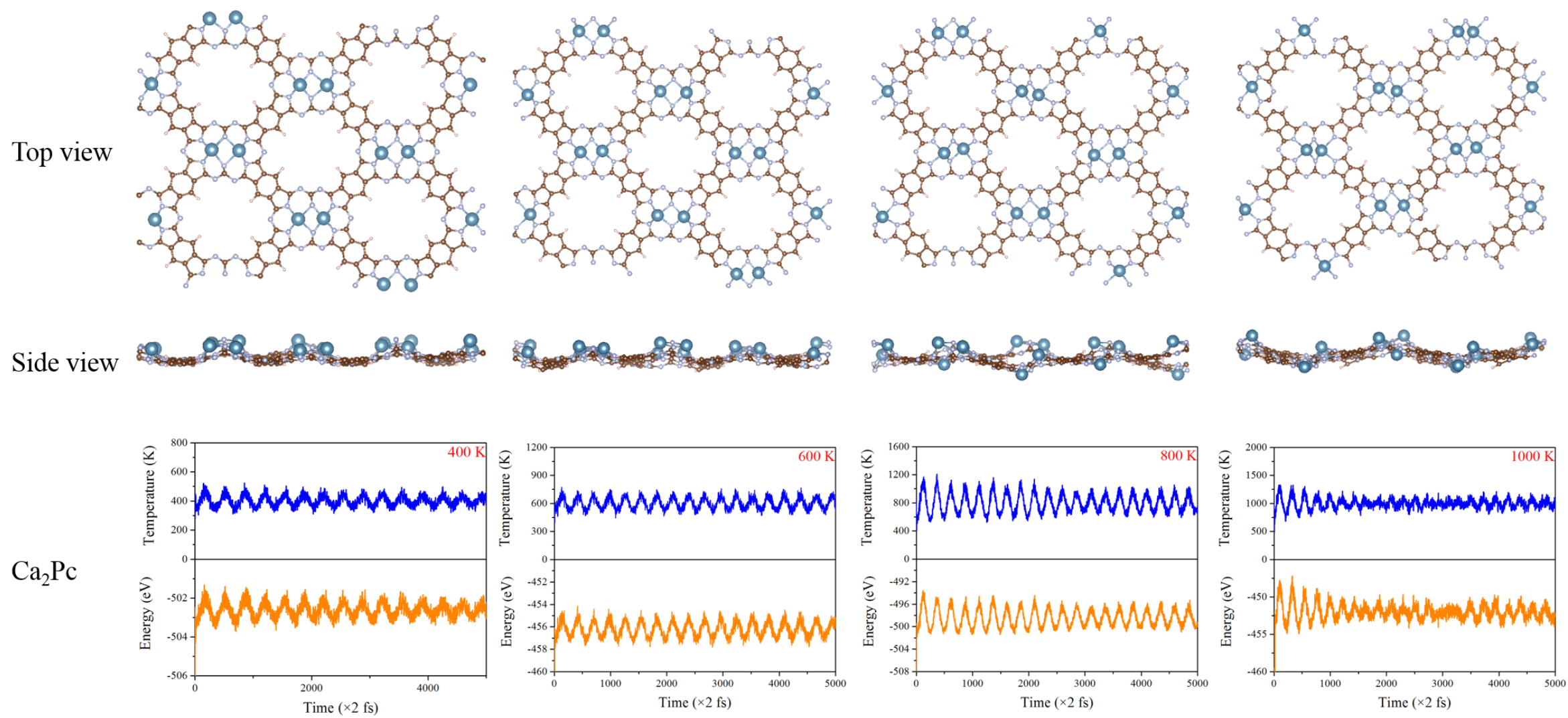


**Figure S3.** AIMD simulations results (include the final snapshot, the evolution of total energy and temperature versus the simulation time) for the  $\text{Ca}_2\text{Pc}$  monolayers at 400, 600 800 and 1000 K, respectively.

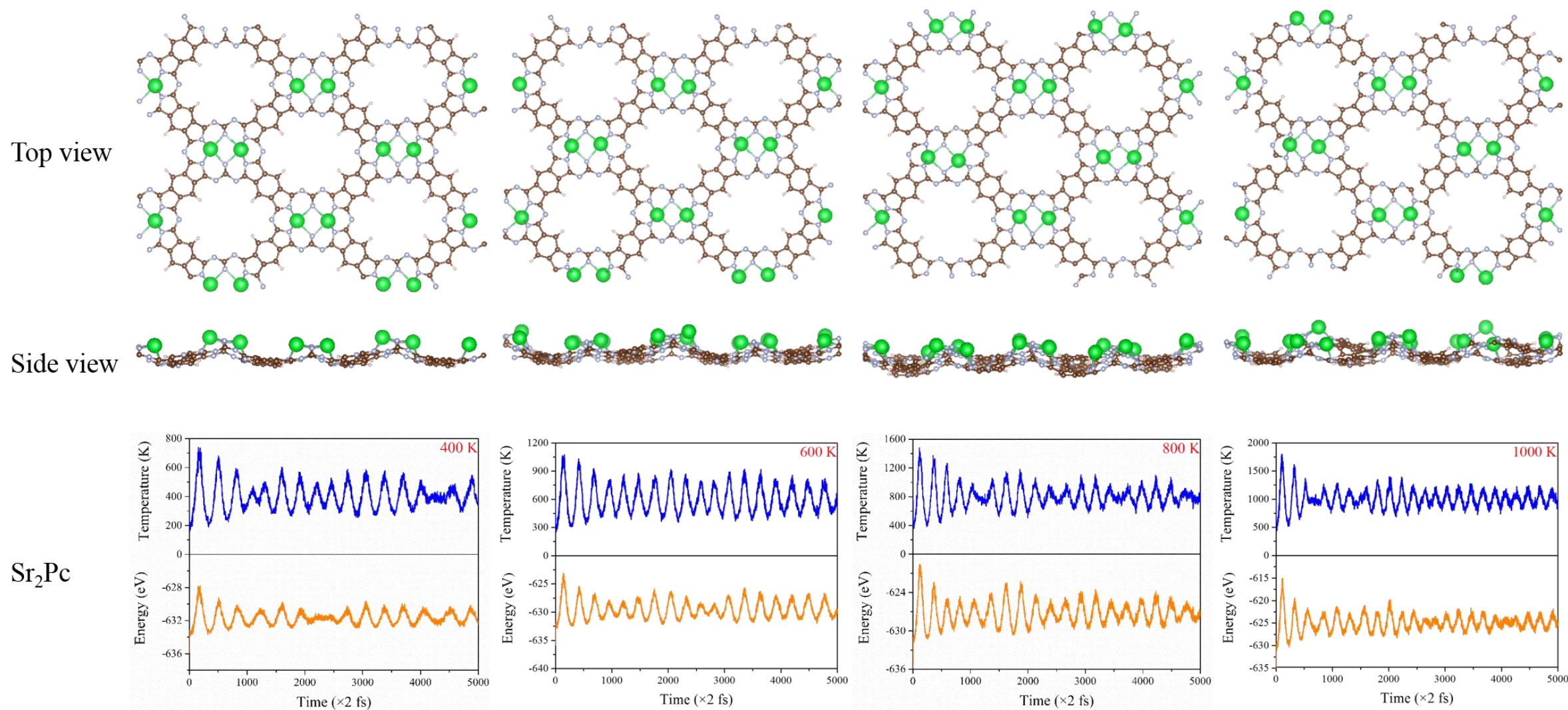


**Figure S4.** AIMD simulations results (include the final snapshot, the evolution of total energy and temperature versus the simulation time) for the  $\text{Sr}_2\text{Pc}$  monolayers at 400, 600 800 and 1000 K, respectively.

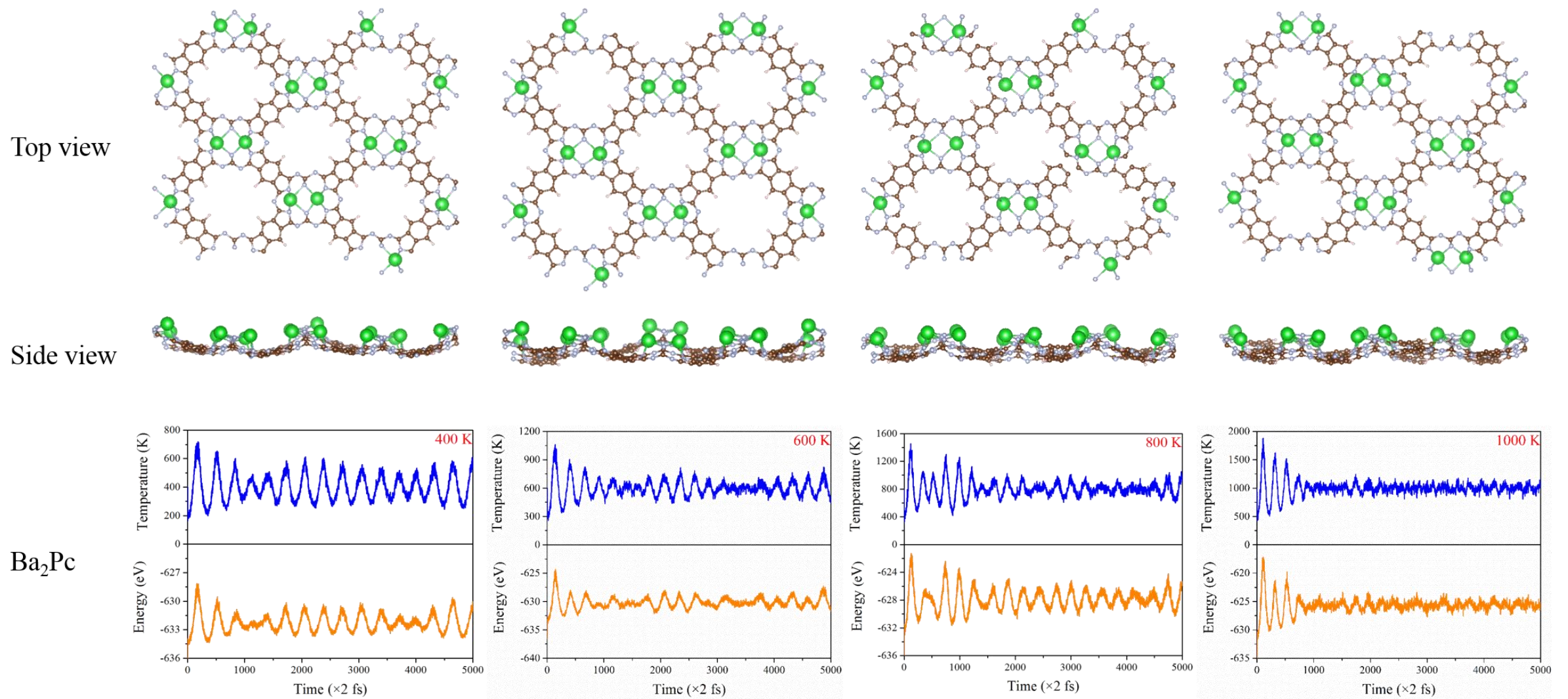


**Figure S5.** AIMD simulations results (include the final snapshot, the evolution of total energy and temperature versus the simulation time) for the Ba<sub>2</sub>Pc monolayers at 400, 600 800 and 1000 K, respectively.

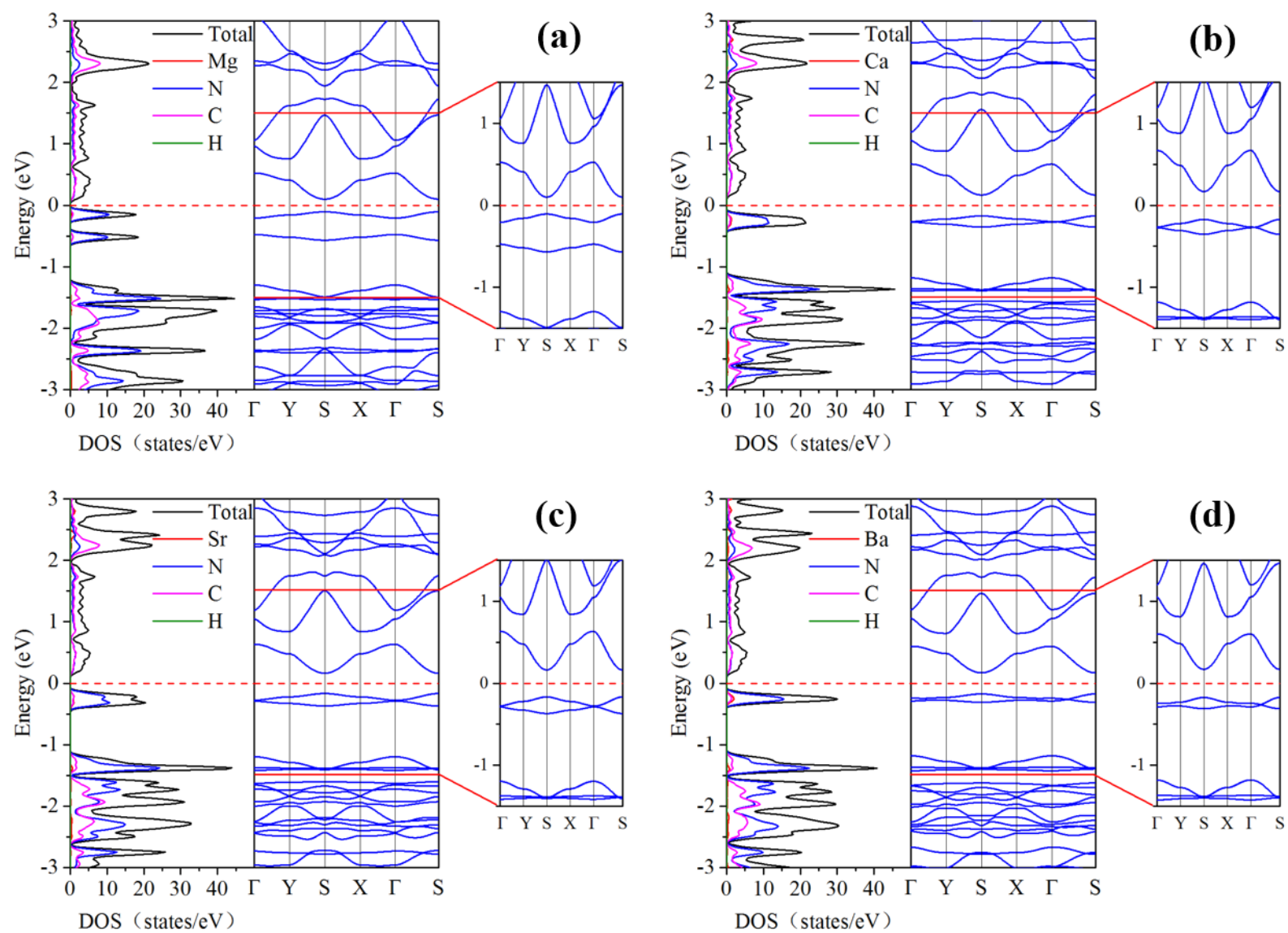


**Figure S6.** Calculated electronic band structures and corresponding total density of states (DOS) based for (a) Mg<sub>2</sub>Pc, (b) Ca<sub>2</sub>Pc, (c) Sr<sub>2</sub>Pc and (d) Ba<sub>2</sub>Pc monolayers at the PBE level. The Fermi level ( $E_F$ ) is set to zero and marked with the dotted line.



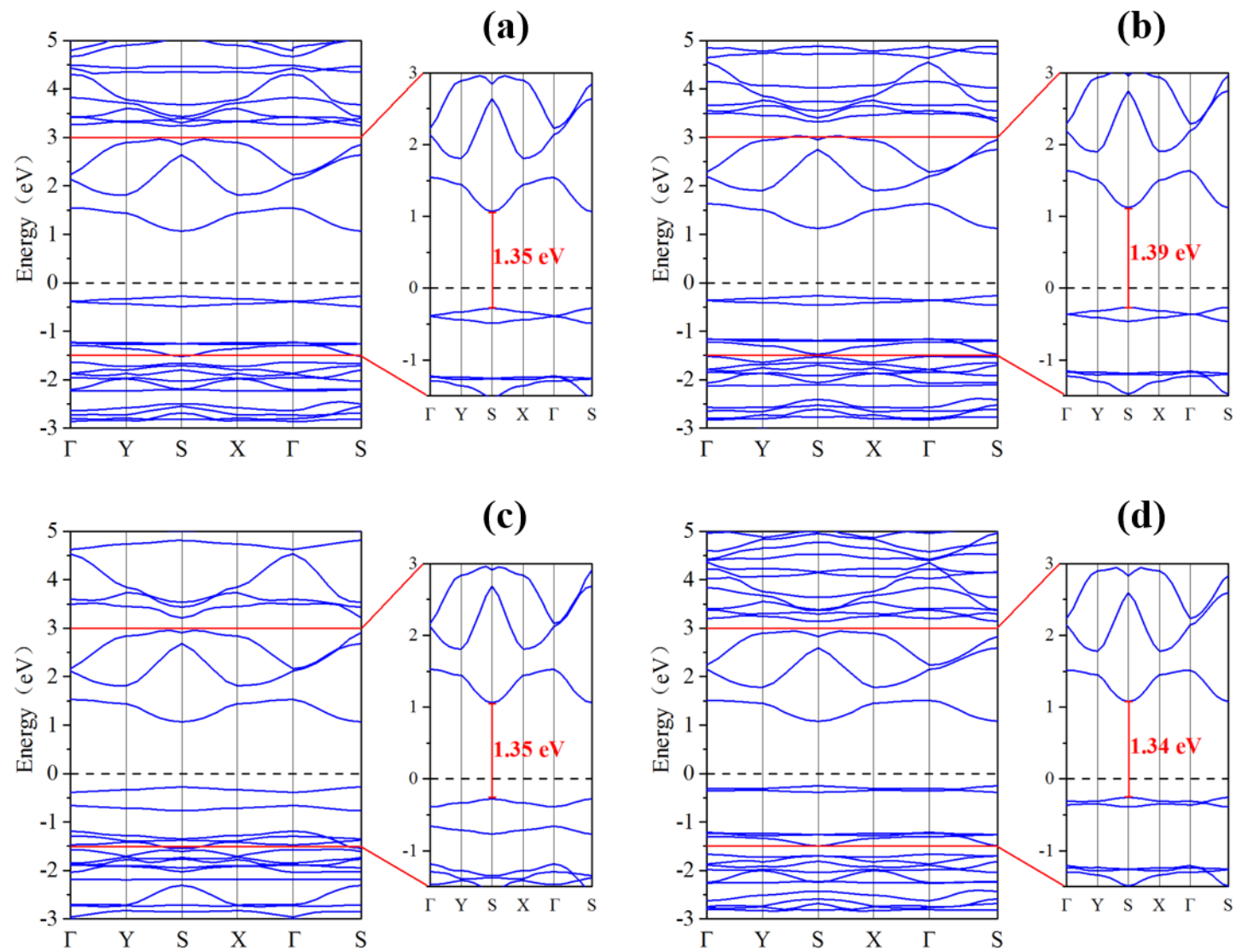


**Figure S7.** Calculated band structures of (a)  $\text{Mg}_2\text{Pc}$ , (b)  $\text{Ca}_2\text{Pc}$ , (c)  $\text{Sr}_2\text{Pc}$  and (d)  $\text{Ba}_2\text{Pc}$  monolayers at the HSE06 level. The Fermi level is set at 0 eV.

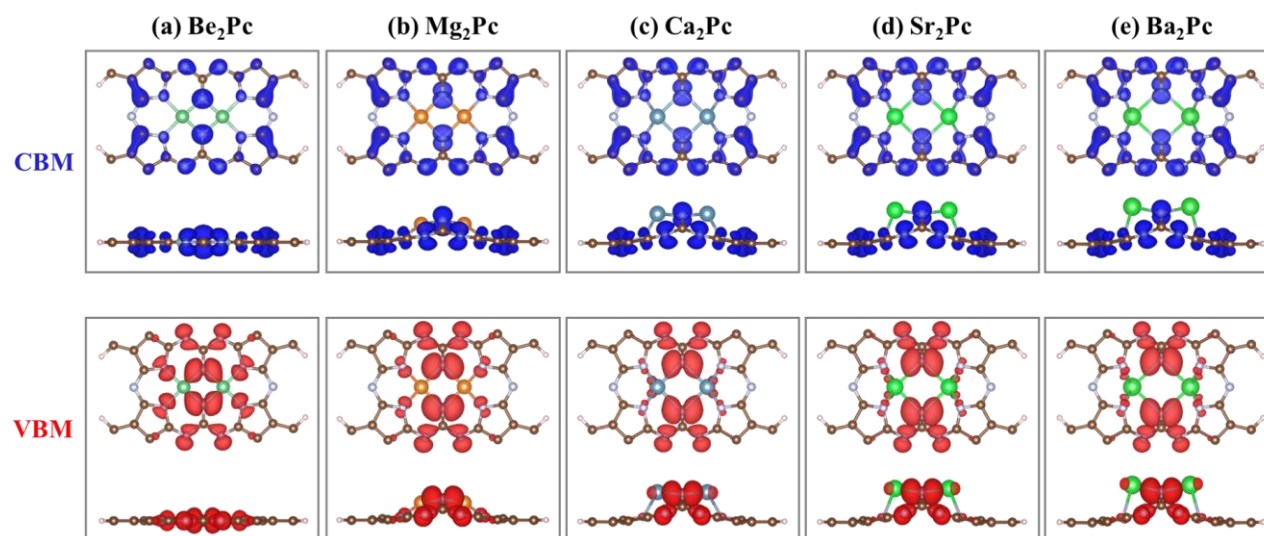


**Figure S8.** The partial charge density distribution of the CBM (blue) and VBM (red) for the  $\text{M}_2\text{Pc}$  monolayers. The isosurface value is  $0.003 \text{ e}/\text{Bohr}^3$ .

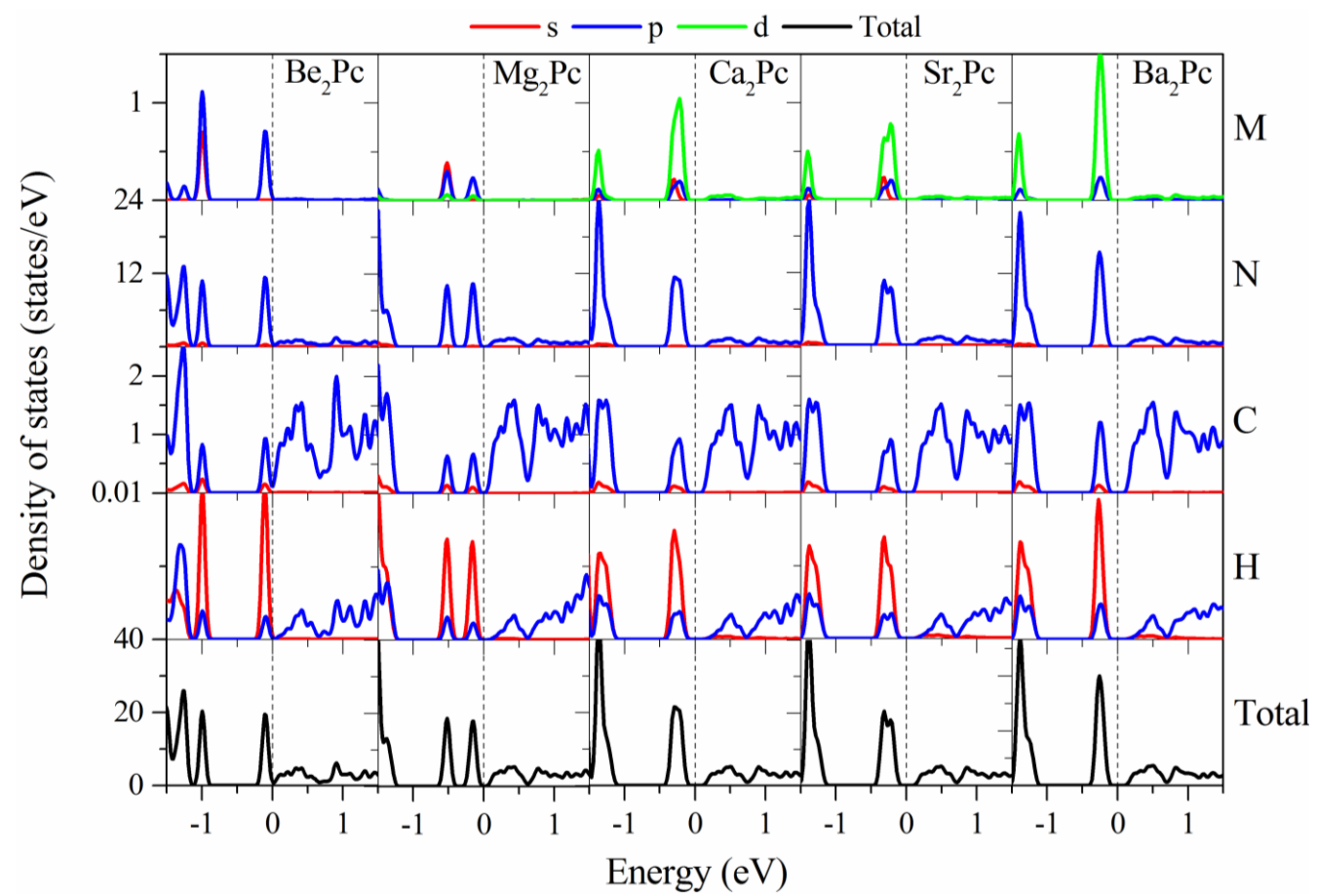


**Figure S9.** Calculated PDOS of the 2D M<sub>2</sub>Pc monolayers in the range of -1.5 to 1.5 eV. Rows represent the PDOS contributions from different types of atoms. The last row shows TDOS for each material.

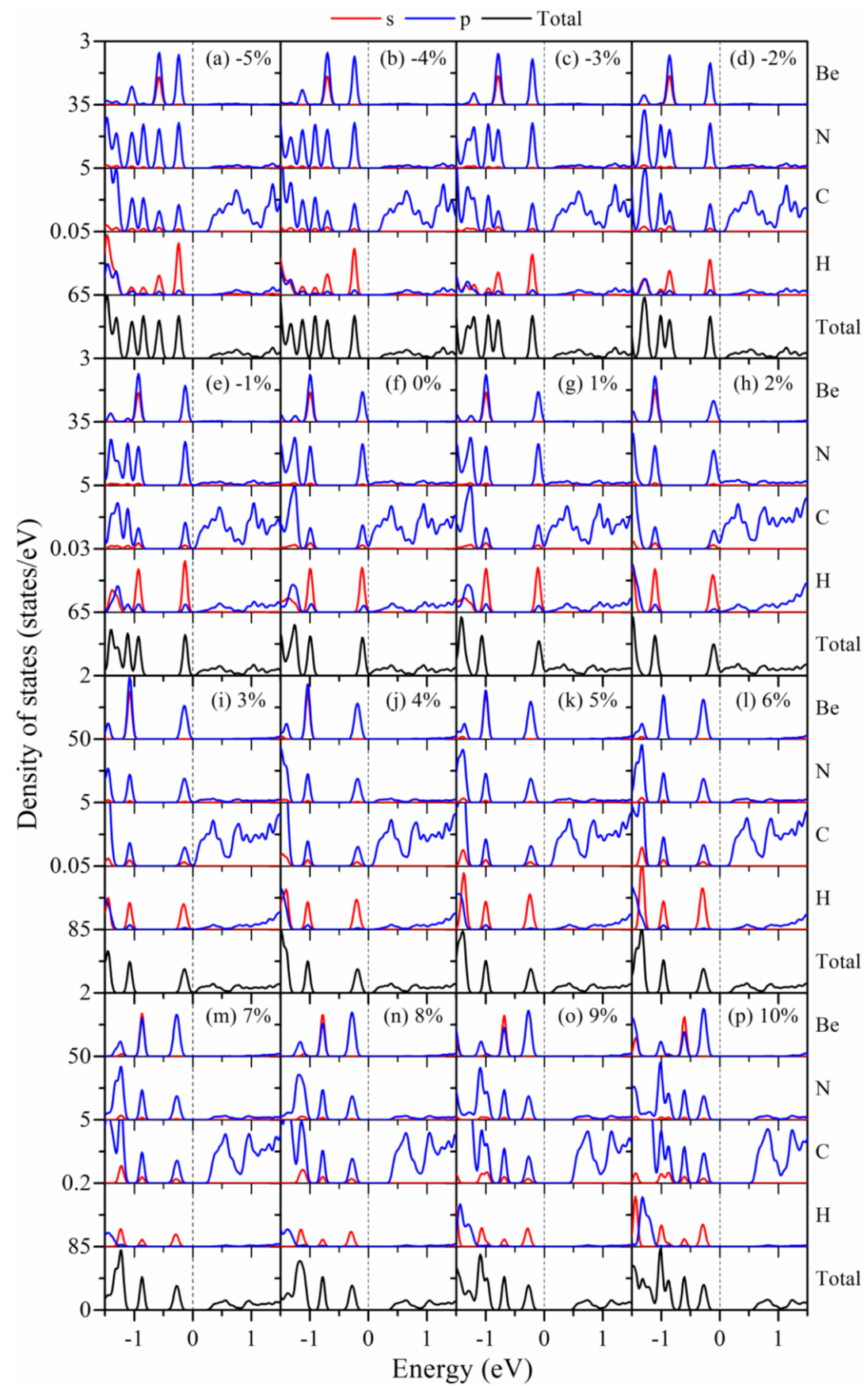


**Figure S10.** The evolution of PDOS on different atoms near the Fermi level versus biaxial strain from  $-5\%$  to  $10\%$  for  $\text{Be}_2\text{Pc}$  monolayer. The Fermi level has been set to  $0$  eV.

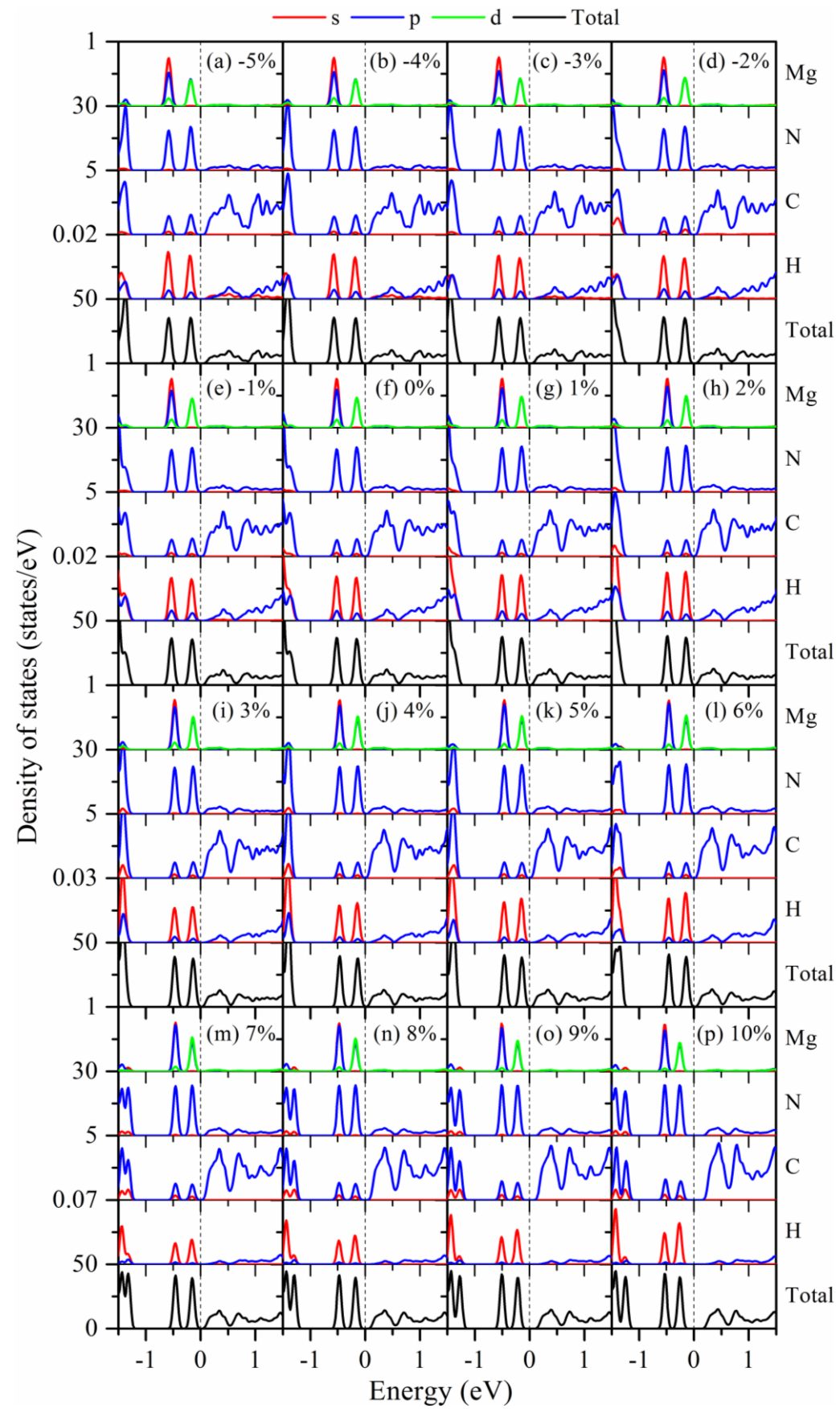


**Figure S11.** The evolution of PDOS on different atoms near the Fermi level versus biaxial strain from  $-5\%$  to  $10\%$  for  $\text{Mg}_2\text{Pc}$  monolayer. The Fermi level has been set to  $0$  eV.

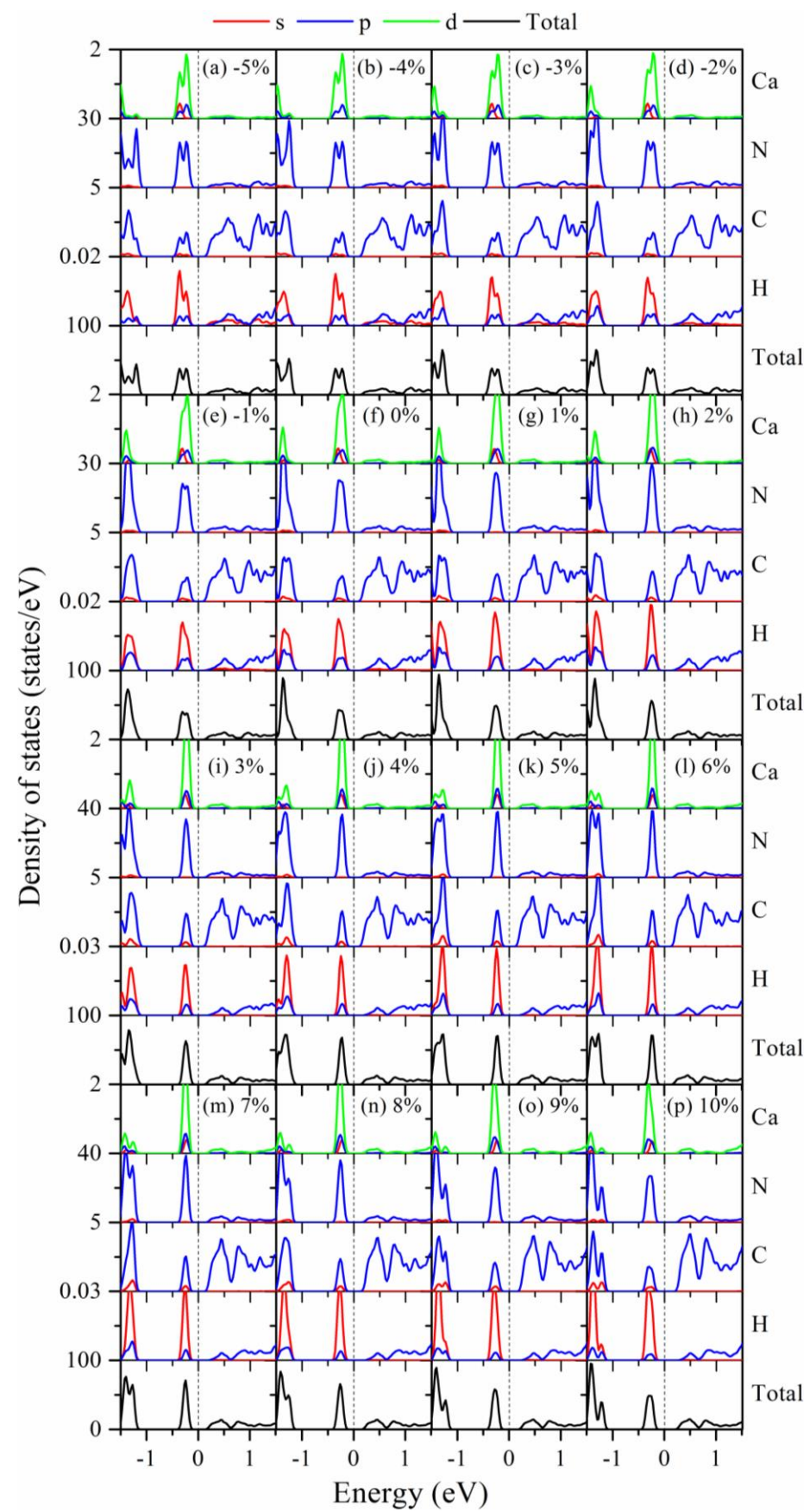


**Figure S12.** The evolution of PDOS on different atoms near the Fermi level versus biaxial strain from -5% to 10% for Ca<sub>2</sub>Pc monolayer. The Fermi level has been set to 0 eV.

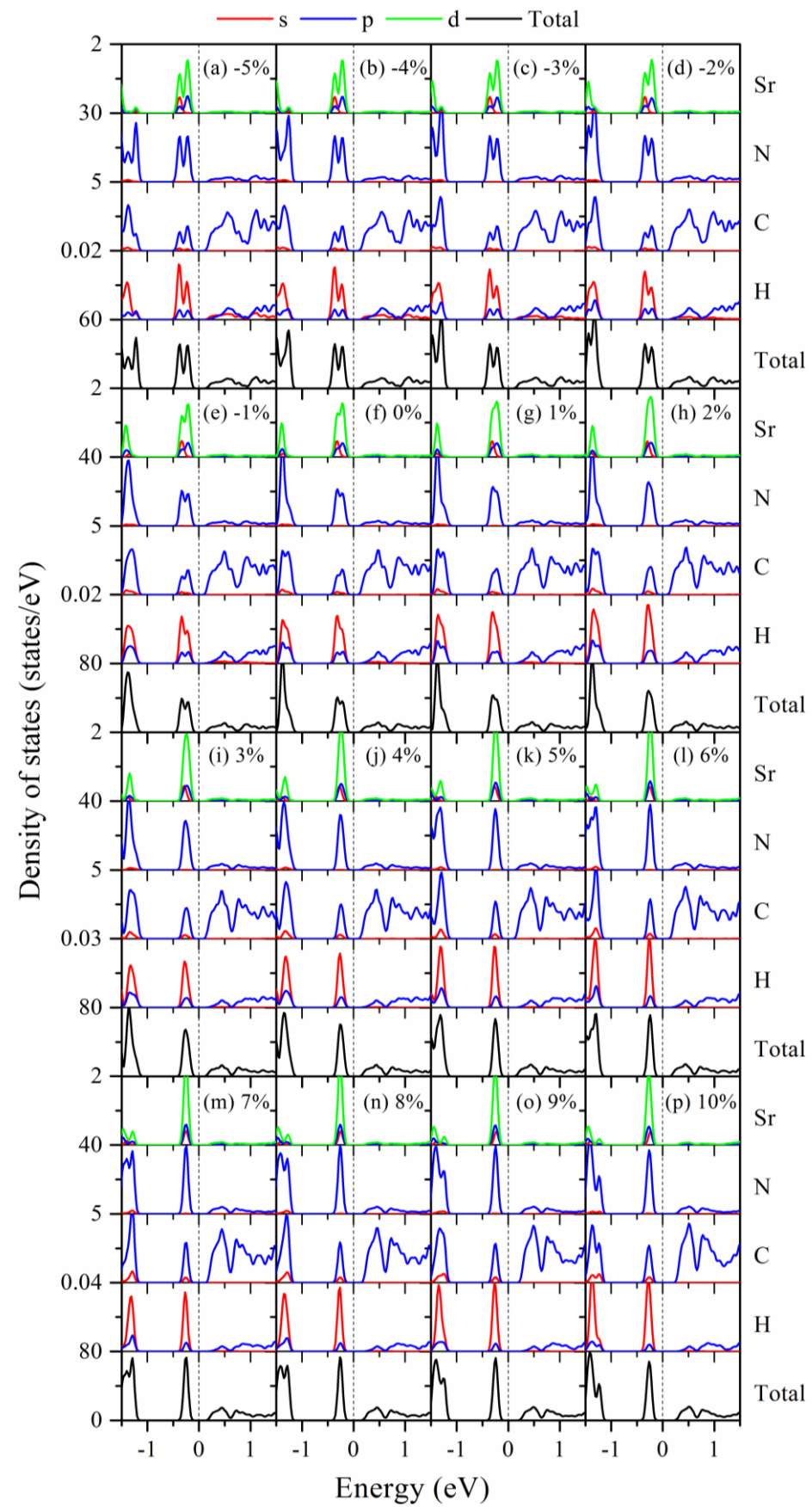


**Figure S13.** The evolution of PDOS on different atoms near the Fermi level versus biaxial strain from  $-5\%$  to  $10\%$  for  $\text{Sr}_2\text{Pc}$  monolayer. The Fermi level has been set to  $0$  eV.

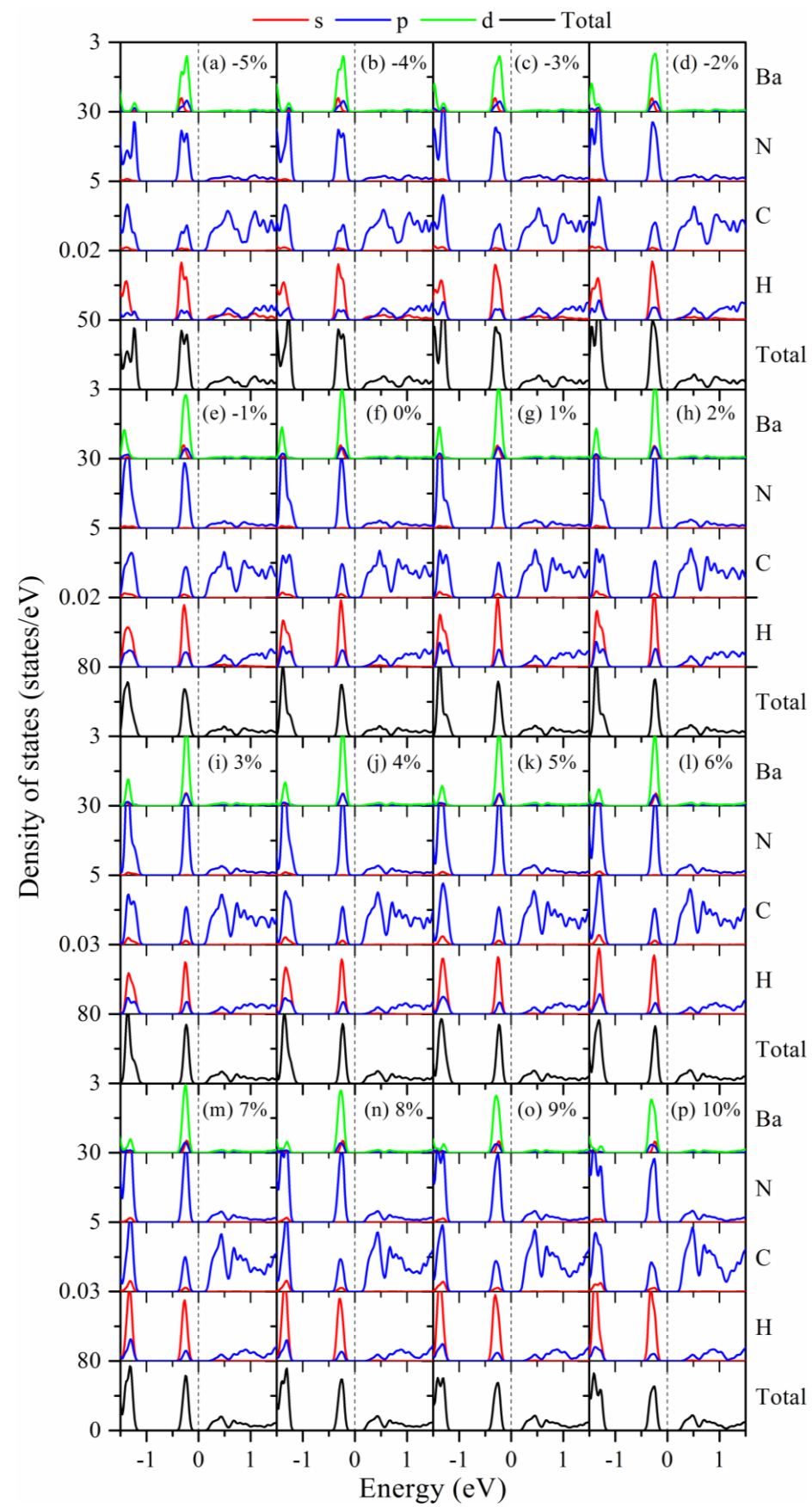


**Figure S14.** The evolution of PDOS on different atoms near the Fermi level versus biaxial strain from -5% to 10% for Ba<sub>2</sub>Pc monolayer. The Fermi level has been set to 0 eV.